
Graph Edit Distance with General Costs Using Neural Set Divergence

Anonymous Author(s)

Affiliation

Address

email

Abstract

1 Graph Edit Distance (GED) measures the (dis-)similarity between two given graphs,
2 in terms of the minimum-cost edit sequence that transforms one graph to the
3 other. However, the exact computation of GED is NP-Hard, which has recently
4 motivated the design of neural methods for GED estimation. However, they do not
5 explicitly account for edit operations with different costs. In response, we propose
6 GRAPHEDX, a neural GED estimator that can work with general costs specified
7 for the four edit operations, *viz.*, edge deletion, edge addition, node deletion and
8 node addition. We first present GED as a quadratic assignment problem (QAP)
9 that incorporates these four costs. Then, we represent each graph as a set of node
10 and edge embeddings and use them to design a family of neural set divergence
11 surrogates. We replace the QAP terms corresponding to each operation with their
12 surrogates. Computing such neural set divergence require aligning nodes and
13 edges of the two graphs. We learn these alignments using a Gumbel-Sinkhorn
14 permutation generator, additionally ensuring that the node and edge alignments
15 are consistent with each other. Moreover, these alignments are cognizant of both
16 the presence and absence of edges between node-pairs. Experiments on several
17 datasets, under a variety of edit cost settings, show that GRAPHEDX consistently
18 outperforms state-of-the-art methods and heuristics in terms of prediction error.

19 1 Introduction

20 The Graph Edit Distance (GED) between a source graph, G , and a target graph, G' , quantifies the
21 minimum cost required to transform G into a graph isomorphic to G' . This transformation involves a
22 sequence of edit operations, which can include node and edge insertions, deletions and substitutions.
23 Each type of edit operation may incur a different and distinctive cost, allowing the GED framework
24 to incorporate domain-specific knowledge. Its flexibility has led to the widespread use of GED for
25 comparing graphs across diverse applications including graph retrieval [5, 6], pattern recognition [46],
26 image and video indexing [50, 48] and chemoinformatics [21]. Because costs for addition and deletion
27 may differ, GED is not necessarily symmetric, *i.e.*, $\text{GED}(G, G') \neq \text{GED}(G', G)$. This flexibility
28 allows GED to model a variety of graph comparison scenarios, such as finding the Maximum Common
29 Subgraph and checking for Subgraph Isomorphism [13]. In general, it is hard to even approximate
30 GED [32]. Recent work [5, 6, 19, 55, 39] has leveraged graph neural networks (GNNs) to build
31 neural models for GED computation, but many of these approaches cannot account for edit operations
32 with different costs. Moreover, several approaches [40, 31, 55, 6] cast GED as the Euclidean distance
33 between graph embeddings, leading to models that are overly attuned to cost-invariant edit sequences.

34 1.1 Present work

35 We propose a novel neural model for computing GED, designed to explicitly incorporate the various
36 costs of edit operations. Our contributions are detailed as follows.

Submitted to 38th Conference on Neural Information Processing Systems (NeurIPS 2024). Do not distribute.

37 **Neural set divergence surrogates for GED** We formulate GED under general (non-uniform) cost
 38 as a quadratic assignment problem (QAP) with four asymmetric distance terms representing edge
 39 deletion, edge addition, node deletion and node addition. The edge-edit operations involve quadratic
 40 dependencies on a node alignment plan — a proposed mapping of nodes from the source graph to
 41 the target graph. To avoid the the complexity of QAP [44], we design a family of differentiable set
 42 divergence surrogates, which can replace the QAP objective with a more benign one. In this approach,
 43 each graph is represented as a set of embeddings of nodes and node-pairs (edges or non-edges). We
 44 replace the original QAP distance terms with their corresponding set divergences, and obtain the node
 45 alignment from a differentiable alignment generator modeled using a Gumbel-Sinkhorn network.
 46 This network produces a soft node permutation matrix based on contextual node embeddings from the
 47 graph pairs, enabling the computation of the overall set divergence in a differentiable manner, which
 48 facilitates end-to-end training. Our proposed model relies on late interaction, where the interactions
 49 between the graph pairs occur only at the final layer, rather than during the embedding computation
 50 in the GNN. This supports the indexing of embedding vectors, thereby facilitating efficient retrieval
 51 through LSH [25, 24, 12], inverted index [20], graph based ANN [34, 37] etc.

52 **Learning all node-pair representations** The optimal sequence of edits in GED is heavily in-
 53 fluenced by the global structure of the graphs. A perturbation in one part of the graph can have
 54 cascading effects, necessitating edits in distant areas. To capture this sensitivity to structural changes,
 55 we associate both edges as well as non-edges with suitable expressive embeddings that capture the
 56 essence of subgraphs surrounding them. Note that the embeddings for non-edges are never explicitly
 57 computed during GNN message-passing operations. They are computed only once, after the GNN
 58 has completed its usual message-passing through *existing* edges, thereby minimizing additional
 59 computational overhead.

60 **Node-edge consistent alignment** To ensure edge-consistency in the learned node alignment map,
 61 we explicitly compute the node-pair alignment map from the node alignment map and then utilize this
 62 derived map to compute collective edge deletion and addition costs. More precisely, if $(u, v) \in G$
 63 and $(u', v') \in G'$ are matched, then the nodes u and v are constrained to match with u' and v' (or, v'
 64 and u') respectively. We call our neural framework as GRAPHEDX.

65 Our experiments across several real datasets show that (1) GRAPHEDX outperforms several state-of-
 66 the-art methods including those that use early interaction; (2) the performance of current state-of-
 67 the-art methods improves significantly when their proposed distance measures are adjusted to reflect
 68 GED-specific distances, as in our approach.

69 2 Problem setup

70 **Notation** The source graph is denoted by $G = (V, E)$ and the target graph by $G' = (V', E')$. Both
 71 graphs are undirected and are padded with isolated nodes to equalize the number of nodes to N .
 72 The adjacency matrices for G and G' after padding are $A, A' \in \{0, 1\}^{N \times N}$. (Note that we will use
 73 M^T , not M' , for the transpose of matrix M .) The sets of padded nodes in G and G' are denoted by
 74 PaddedNodes_G and $\text{PaddedNodes}_{G'}$ respectively. We construct $\eta \in \{0, 1\}^N$, where $\eta[u] = 0$ if
 75 $u \in \text{PaddedNodes}_G$ and 1 otherwise (same for G'). The embedding of a node $u \in V$ computed at
 76 propagation layer k by the GNN, is represented as $x_k(u)$. Edit operations, denoted by edit , belong to
 77 one of four types, *viz.*, (i) node deletion, (ii) node addition, (iii) edge deletion, (iv) edge addition. Each
 78 operation edit is assigned a cost $\text{cost}(\text{edit})$. The node and node-pair alignment maps are described
 79 using (hard) permutation matrices $P \in \{0, 1\}^{N \times N}$ and $S \in \{0, 1\}^{\binom{N}{2} \times \binom{N}{2}}$ respectively. Given that
 80 the graphs are undirected, node-pair alignment need only be specified across at most $\binom{N}{2}$ pairs. When
 81 a hard permutation matrix is relaxed to a doubly-stochastic matrix, we call it a soft permutation
 82 matrix. We use P and S to refer to both hard and soft permutations, depending on the context. We
 83 denote \mathbb{P}_N as the set of all hard permutation matrices of dimension N ; $[N]$ as $\{1, \dots, N\}$ and $\|A\|_{1,1}$
 84 to describe $\sum_{u,v} |A[u, v]|$. For two binary variables $c_1, c_2 \in \{0, 1\}$, we denote $J(c_1, c_2)$ as $(c_1 \text{ XOR}$
 85 $c_2)$, *i.e.*, $J(c_1, c_2) = c_1 c_2 + (1 - c_1)(1 - c_2)$.

86 **Graph edit distance with general cost** We define an *edit path* as a sequence of edit operations
 87 $\mathcal{o} = \{\text{edit}_1, \text{edit}_2, \dots\}$; and $\mathcal{O}(G, G')$ as the set of all possible edit paths that transform the source
 88 graph G into a graph isomorphic to the target graph G' . Given $\mathcal{O}(G, G')$ and the cost associated with
 89 each operation edit , the GED between G and G' is the minimum collective cost across all edit paths

90 in $\mathcal{O}(G, G')$. Formally, we write [14, 7]:

$$\text{GED}(G, G') = \min_{\sigma=\{\text{edit}_1, \text{edit}_2, \dots\} \in \mathcal{O}(G, G')} \sum_{i \in [|\sigma|]} \text{cost}(\text{edit}_i). \quad (1)$$

91 In this work, we assume a fixed cost for each of the four types of edit operations. Specifically, we use
 92 a^\ominus , a^\oplus , b^\ominus and b^\oplus to represent the costs for edge deletion, edge addition, node deletion, and node
 93 addition, respectively. These costs are not necessarily equal, in contrast to the assumptions made in
 94 previous works [5, 31, 55, 39]. Additional discussion on GED with node substitution in presence of
 95 labels can be found in Appendix D.

96 **Problem statement** Our objective is to design a neural architecture for predicting GED under
 97 a general cost framework, where the edit costs a^\ominus , a^\oplus , b^\ominus and b^\oplus are not necessarily the same.
 98 During the learning stage, these four costs are specified, and remain fixed across all training instances
 99 $\mathcal{D} = \{(G_i, G'_i, \text{GED}(G_i, G'_i))\}_{i \in [n]}$. Note that the edit paths are not supervised. Later, given a test
 100 instance G, G' , assuming the same four costs, the trained system has to predict $\text{GED}(G, G')$.

101 3 Proposed approach

102 In this section, we first present an alternative formulation of GED as described in Eq. (1), where
 103 the edit paths are induced by node alignment maps. Then, we adapt this formulation to develop
 104 GRAPHEDX, a neural set distance surrogate, amenable to end-to-end training. Finally, we present the
 105 network architecture of GRAPHEDX.

106 3.1 GED computation using node alignment map

107 Given the padded graph pair G and G' , deleting a node $u \in V$ can be viewed as aligning node u
 108 with some padded node $u' \in \text{PaddedNodes}_{G'}$. Similarly, adding a new node u' to G can be seen as
 109 aligning some padded node $u \in \text{PaddedNodes}_G$ with node $u' \in V'$. Likewise, adding an edge to G
 110 corresponds to aligning a non-edge $(u, v) \notin E$ with an edge $(u', v') \in G'$. Conversely, deleting an
 111 edge in G corresponds to aligning an edge $(u, v) \in G$ with a non-edge $(u', v') \notin G'$.

112 Therefore, $\text{GED}(G, G')$ can be defined in terms of a node alignment map. Let Π_N represent the set of
 113 all node alignment maps $\pi : [N] \rightarrow [N]$ from V to V' . Recall that $\eta_G[u] = 0$ if $u \in \text{PaddedNodes}_G$
 114 and 1 otherwise.

$$\min_{\pi \in \Pi_N} \frac{1}{2} \sum_{u, v} \left(a^\ominus \cdot \mathbb{I}[(u, v) \in E \wedge (\pi(u), \pi(v)) \notin E'] + a^\oplus \cdot \mathbb{I}[(u, v) \notin E \wedge (\pi(u), \pi(v)) \in E'] \right) \\ + \sum_u \left(b^\ominus \cdot \eta_G[u] (1 - \eta_{G'}[\pi(u)]) + b^\oplus \cdot (1 - \eta_G[u]) \eta_{G'}[\pi(u)] \right). \quad (2)$$

115 In the above expression, the first sum iterates over all pairs of $(u, v) \in [N] \times [N]$ and the second
 116 sum iterates over $u \in [N]$. Because both graphs are undirected, the fraction $1/2$ accounts for double
 117 counting of the edges. The first and second terms quantify the cost of deleting and adding the edge
 118 (u, v) from and to G , respectively. The third and the fourth terms evaluate the cost of deleting and
 119 adding node u from and to G , respectively.

120 **GED as a quadratic assignment problem** In its current form, Eq. (2) cannot be immediately
 121 adapted to a differentiable surrogate. To circumvent this problem, we provide an equivalent matricized
 122 form of Eq. (2), using a hard node permutation matrix P instead of the alignment map π . We compute
 123 the asymmetric distances between A and $PA'P^\top$ and combine them with weights a^\ominus and a^\oplus .
 124 Notably, $\text{ReLU}(A - PA'P^\top)[u, v]$ is non-zero if the edge $(u, v) \in E$ is mapped to a non-edge
 125 $(u', v') \in E'$ with $P[u, u'] = P[v, v'] = 1$, indicating deletion of the edge (u, v) from G . Similarly,
 126 $\text{ReLU}(PA'P^\top - A)[u, v]$ becomes non-zero if an edge (u, v) is added to G . Therefore, for the
 127 edit operations involving edges, we have:

$$\mathbb{I}[(u, v) \in E \wedge (\pi(u), \pi(v)) \notin E'] = \text{ReLU}(A - PA'P^\top)[u, v], \quad (3)$$

$$\mathbb{I}[(u, v) \notin E \wedge (\pi(u), \pi(v)) \in E'] = \text{ReLU}(PA'P^\top - A)[u, v]. \quad (4)$$

128 Similarly, we note that $\text{ReLU}(\eta_G[u] - \eta_{G'}[\pi(u)]) > 0$ if $u \notin \text{PaddedNodes}_G$ and $\pi(u) \in$
 129 $\text{PaddedNodes}_{G'}$, which allows us to compute the cost of deleting the node u from G . Similarly, we
 130 use $\text{ReLU}(\eta_{G'}[\pi(u)] - \eta_G[u])$ to account for the addition of the node u to G . Formally, we write:

$$\eta_G[u] (1 - \eta_{G'}[\pi(u)]) = \text{ReLU}(\eta_G[u] - \eta_{G'}[\pi(u)]), \quad (5)$$

$$(1 - \eta_G[u]) \eta_{G'}[\pi(u)] = \text{ReLU}(\eta_{G'}[\pi(u)] - \eta_G[u]). \quad (6)$$

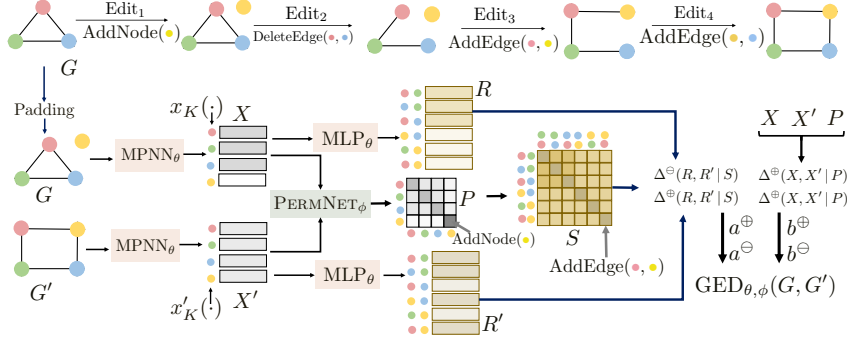


Figure 1: **Top:** Example graphs G and G' are shown with color-coded nodes to indicate alignment corresponding to the optimal edit path transforming G to G' . **Bottom:** GRAPHEDX’s GED prediction pipeline. G and G' are independently encoded using MPNN_θ , and then padded with zero vectors to equalize sizes, resulting in contextual node representations $X, X' \in \mathbb{R}^{N \times d}$. For each node-pair, the corresponding embeddings and edge presence information are gathered and fed into MLP_θ to obtain $R, R' \in \mathbb{R}^{N(N-1)/2 \times D}$. Simultaneously, X, X' are fed into PERMNET_ϕ to obtain the soft node alignment P (Eq.(18)) which constructs the node-pair alignment matrix $S \in \mathbb{R}^{N(N-1)/2 \times N(N-1)/2}$ as $S[u, v], (u', v')] = P[u, u']P[v, v'] + P[u, v']P[v, u']$. Finally, X, X', P are used to approximate node insertion and deletion costs, while R, R', S are used to approximate edge insertion and deletion costs. The four costs are summed to give the final prediction $\text{GED}_{\theta, \phi}(G, G')$ (Eq.(9)).

131 Using Eqs. (3)–(6), we rewrite Eq. (2) as:

$$\text{GED}(G, G') = \min_{P \in \mathbb{P}_N} \frac{a^\ominus}{2} \|\text{ReLU}(A - PA'P^\top)\|_{1,1} + \frac{a^\oplus}{2} \|\text{ReLU}(PA'P^\top - A)\|_{1,1} \\ + b^\ominus \|\text{ReLU}(\eta_G - P\eta_{G'})\|_1 + b^\oplus \|\text{ReLU}(P\eta_{G'} - \eta_G)\|_1. \quad (7)$$

132 The first and the second term denote the collective costs of deletion and addition of edges, respectively.
 133 The third and the fourth terms present a matricized representation of Eqs. (5)- (6). The above problem
 134 can be viewed as a quadratic assignment problem (QAP) on graphs, given that the hard node
 135 permutation matrix P has a quadratic involvement in the first two terms. Note that, in general,
 136 $\text{GED}(G, G') \neq \text{GED}(G', G)$. However, the optimal edit paths for these two GED values, encoded
 137 by the respective node permutation matrices, are inverses of each other, as formally stated in the
 138 following proposition (proven in Appendix D).

139 **Proposition 1** Given a fixed set of values of $b^\ominus, b^\oplus, a^\ominus, a^\oplus$, let P be an optimal node permutation
 140 matrix corresponding to $\text{GED}(G, G')$, computed using Eq. (7). Then, $P' = P^\top$ is an optimal node
 141 permutation corresponding to $\text{GED}(G', G)$.

142 **Connection to different notions of graph matching** The above expression of GED can be used
 143 to represent various notions of graph matching and similarity measures by modifying the edit costs.
 144 These include graph isomorphism, subgraph isomorphism, and maximum common edge subgraph
 145 detection. For example, by setting all costs to one, $\text{GED}(G, G') = \min_P \frac{1}{2} \|A - PA'P^\top\|_1 + \|\eta_G -$
 146 $P\eta_{G'}\|_1$, which equals zero only when G and G' are isomorphic. Further discussion on this topic is
 147 provided in Appendix D.

148 3.2 GRAPHEDX model

149 Minimizing the objective in Eq. (7) is a challenging problem. In similar problems, recent methods
 150 have approximated the hard node permutation matrix P with a soft permutation matrix obtained
 151 using Sinkhorn iterations on a neural cost matrix. However, the binary nature of the adjacency matrix
 152 and the pad indicator q still impede the flow of gradients during training. To tackle this problem, we
 153 make relaxations in two key places within each term in Eq. (7), leading to our proposed GRAPHEDX
 154 model.

155 (1) We replace the binary values in $q_G, q_{G'}, A$ and A' with real values from node and node-pair
 156 embeddings: $X \in \mathbb{R}^{N \times d}$ and $R \in \mathbb{R}^{\binom{N}{2} \times D}$. These embeddings are computed using a GNN
 157 guided neural module EMBED_θ with parameter θ . Since the graphs are undirected, R gathers the
 158 embeddings of the unique node-pairs, resulting in $\binom{N}{2}$ rows instead of N^2 .

159 (2) We substitute the hard node permutation matrix P with a soft alignment matrix, generated using
 160 a differentiable alignment planner PERMNET_ϕ with parameter ϕ . Here, P is a doubly stochastic
 161 matrix, with $P[u, u']$ indicating the "score" or "probability" of aligning $u \mapsto u'$. Additionally,
 162 we also compute the corresponding node-pair alignment matrix S .

163 Using these relaxations, we approximate the four edit costs in Eq. (7) with four continuous set
 164 distance surrogate functions.

$$\begin{aligned} \|\text{ReLU}(A - PA'P^\top)\|_{1,1} &\rightarrow \Delta^\ominus(R, R' | S), & \|\text{ReLU}(PA'P^\top - A)\|_{1,1} &\rightarrow \Delta^\oplus(R, R' | S), \\ \|\text{ReLU}(\eta_G - P\eta_{G'})\|_1 &\rightarrow \Delta^\ominus(X, X' | P), & \|\text{ReLU}(P\eta_{G'} - \eta_G)\|_1 &\rightarrow \Delta^\oplus(X, X' | P). \end{aligned} \quad (8)$$

165 This gives us an approximated GED parameterized by θ and ϕ .

$$\begin{aligned} \text{GED}_{\theta, \phi}(G, G') &= a^\ominus \Delta^\ominus(R, R' | S) + a^\oplus \Delta^\oplus(R, R' | S) \\ &\quad + b^\ominus \Delta^\ominus(X, X' | P) + b^\oplus \Delta^\oplus(X, X' | P). \end{aligned} \quad (9)$$

166 Note that since R and R' contain the embeddings of each node-pair only once, there is no need to
 167 multiply $1/2$ in the first two terms, unlike Eq. (7). Next, we propose three types of neural surrogates
 168 to approximate each of the four operations.

169 **(1) AlignDiff** Given the node-pair embeddings R and R' for the graph pairs G and G' , we apply the
 170 soft node-pair alignment S to R' . We then define the edge edits in terms of asymmetric differences
 171 between R and SR' , which serves as a replacement for the corresponding terms in Eq. (7). We write
 172 $\Delta^\ominus(R, R' | S)$ and $\Delta^\oplus(R, R' | S)$ as:

$$\Delta^\ominus(R, R' | S) = \|\text{ReLU}(R - SR')\|_{1,1}, \quad \Delta^\oplus(R, R' | S) = \|\text{ReLU}(SR' - R)\|_{1,1}. \quad (10)$$

173 Similarly, for the node edits, we can compute $\Delta^\ominus(X, X' | P)$ and $\Delta^\oplus(X, X' | P)$ as:

$$\Delta^\ominus(X, X' | P) = \|\text{ReLU}(X - PX')\|_{1,1}, \quad \Delta^\oplus(X, X' | P) = \|\text{ReLU}(PX' - X)\|_{1,1}. \quad (11)$$

174 **(2) DiffAlign** In Eq. (10), we first aligned R' using S and then computed the difference from R .
 175 Instead, here we first computed the pairwise differences between R' and R for all pairs of node-pairs
 176 (e, e') , and then combine these differences with the corresponding alignment scores $S[e, e']$. We
 177 compute the edge edit surrogates $\Delta^\ominus(R, R' | S)$ and $\Delta^\oplus(R, R' | S)$ as:

$$\Delta^\ominus(R, R' | S) = \sum_{e, e'} \|\text{ReLU}(R[e, :] - R'[e', :])\|_1 S[e, e'], \quad (12)$$

$$\Delta^\oplus(R, R' | S) = \sum_{e, e'} \|\text{ReLU}(R'[e', :] - R[e, :])\|_1 S[e, e']. \quad (13)$$

178 Here, e and e' represent node-pairs, which are not necessarily edges. When the node-
 179 pair alignment matrix S is a hard permutation, Δ^\oplus and Δ^\ominus remain the same across
 180 AlignDiff and DiffAlign (as shown in Appendix D). Similar to Eqs. (12)–(13), we can com-
 181 pute $\Delta^\ominus(X, X' | P) = \sum_{u, u'} \|\text{ReLU}(X[u, :] - X'[u', :])\|_1 P[u, u']$ and $\Delta^\oplus(X, X' | P) =$
 182 $\sum_{u, u'} \|\text{ReLU}(X'[u', :] - X[u, :])\|_1 P[u, u']$.

183 **(3) XOR-DiffAlign** As indicated by the combinatorial formulation of GED in Eq. (7), the edit
 184 cost of a particular node-pair is non-zero only when an edge is mapped to a non-edge or vice-versa.
 185 However, the surrogates for the edge edits in AlignDiff or DiffAlign fail to capture this condition
 186 because they can assign non-zero costs to the pairs $(e = (u, v), e' = (u', v'))$ even when both e
 187 and e' are either edges or non-edges. To address this, we explicitly discard such pairs from the
 188 surrogates defined in Eqs. (12)–(13). This is ensured by applying a XOR operator $J(\cdot, \cdot)$ between
 189 the corresponding entries in the adjacency matrices, i.e., $A[u, v]$ and $A'[u', v']$, and then multiplying
 190 this result with the underlying term. Hence, we write:

$$\Delta^\ominus(R, R' | S) = \sum_{e=(u,v)} \sum_{e'=(u',v')} J(A[u, v], A'[u', v']) \|\text{ReLU}(R[e, :] - R'[e', :])\|_1 S[e, e'], \quad (14)$$

$$\Delta^\oplus(R, R' | S) = \sum_{e=(u,v)} \sum_{e'=(u',v')} J(A[u, v], A'[u', v']) \|\text{ReLU}(R'[e', :] - R[e, :])\|_1 S[e, e']. \quad (15)$$

191 Similarly, the cost contribution for node operations arises from mapping a padded node to
 192 a non-padded node or vice versa. We account for this by multiplying $J(\eta_G[u], \eta_{G'}[u'])$
 193 with each term of $\Delta^\ominus(X, X' | P)$ and $\Delta^\oplus(X, X' | P)$ computed using DiffAlign. Hence, we
 194 compute $\Delta^\ominus(X, X' | P) = \sum_{u, u'} J(\eta_G[u], \eta_{G'}[u']) \|\text{ReLU}(X[u, :] - X'[u', :])\|_1 P[u, u']$ and
 195 $\Delta^\oplus(X, X' | P) = \sum_{u, u'} J(\eta_G[u], \eta_{G'}[u']) \|\text{ReLU}(X'[u', :] - X[u, :])\|_1 P[u, u']$.

196 **Comparison between AlignDiff, DiffAlign and XOR-DiffAlign** AlignDiff and DiffAlign be-
 197 come equivalent when S is a hard permutation. However, when S is doubly stochastic, the above
 198 three surrogates, AlignDiff, DiffAlign and XOR-DiffAlign, are not equivalent. As we move from
 199 AlignDiff to DiffAlign to XOR-DiffAlign, we increasingly align the design to the inherent inductive
 200 biases of GED, thereby achieving a better representation of its cost structure.

201 Suppose we are computing the GED between two isomorphic graphs, G and G' , with equal costs
 202 for all edit operations. In this scenario, we ideally expect a neural network to consistently output
 203 a zero cost. Now consider a proposed soft alignment S which is close to the optimal alignment.
 204 Under the AlignDiff design, the aggregated value $\sum_{e'} S[e, e'] R[e', :]$ — where e and e' represent two
 205 edges matched in the optimal alignment — can accumulate over the large number of $N(N-1)/2$
 206 node-pairs. This aggregation leads to high values of $\|R[e, :] - SR'[e', :]\|_1$, implying that AlignDiff
 207 captures an aggregate measure of the cost incurred by spurious alignments, but cannot disentangle
 208 the effect of individual misalignments. This makes it difficult for AlignDiff to learn the optimal
 209 alignment.

210 In contrast, the DiffAlign approach, which relies on pairwise differences between embeddings to
 211 explicitly guide S towards the optimal alignment, significantly ameliorates this issue. For example,
 212 in the aforementioned setting of GED with equal costs, the cost associated with each pairing (e, e')
 213 is explicitly encoded using $\|R[e, :] - R'[e', :]\|_1$, and is explicitly set to zero for pairs that are
 214 correctly aligned. Moreover, this representation allows DiffAlign to isolate the cost incurred by each
 215 misalignment, making it easier to train the model to reduce the cost of these spurious matches to zero.

216 However, DiffAlign does not explicitly set edge-to-edge and non-edge-to-non-edge mapping costs to
 217 zero, potentially leading to inaccurate GED estimates. XOR-DiffAlign addresses these concerns by
 218 applying a XOR of the adjacency matrices to the cost matrix, ensuring that non-zero cost is computed
 219 only when mapping an edge to a non-edge or vice versa. This resolves the issues in both AlignDiff and
 220 DiffAlign by focusing on mismatches between edges and non-edges, while disregarding redundant
 221 alignments that do not contribute to the GED.

222 **Amenability to indexing and approximate nearest neighbor (ANN) search.** All of the aforemen-
 223 tioned distance surrogates are based on a late interaction paradigm, where the embeddings of G and
 224 G' are computed independently of each other before computing the distances Δ . This is particularly
 225 useful in the context of graph retrieval, as it allows for the corpus graph embeddings to be indexed
 226 a-priori, thereby enabling efficient retrieval of relevant graphs for new queries.

227 When the edit costs are equal, our predicted GED (9) becomes symmetric with respect to G and G' .
 228 In such cases, DiffAlign and AlignDiff yield a structure similar to the Wasserstein distance induced
 229 by L_1 norm. This allows us to leverage ANN techniques like Quadtree or Flowtree [4]. However,
 230 while the presence of the XOR operator J within each term in Eq. (14) – (15) of XOR-DiffAlign
 231 enhances the interaction between G and G' , this same feature prevents XOR-DiffAlign from being
 232 cast to an ANN-amenable setup, unlike DiffAlign and AlignDiff.

233 3.3 Network architecture of EMBED_θ and PERMNET_ϕ

234 In this section, we present the network architectures of the two components of GRAPHEDX , *viz.*,
 235 EMBED_θ and PERMNET_ϕ , as introduced in items (1) and (2) in Section 3.2. Notably, in our proposed
 236 graph representation, non-edges and edges alike are embedded as non-zero vectors. In other words,
 237 all node-pairs are endowed with non-trivial embeddings. We then explain the design approach for
 238 edge-consistent node alignment.

239 **Neural architecture of EMBED_θ** EMBED_θ consists of a message passing neural network MPNN_θ
 240 and a decoupled neural module MLP_θ . Given the graphs G, G' , MPNN_θ with K propaga-
 241 tion layers is used to iteratively compute the node embeddings $\{x_K(u) \in \mathbb{R}^d \mid u \in V\}$ and
 242 $\{x'_K(u) \in \mathbb{R}^d \mid u \in V'\}$, then collect them into X and X' after padding, *i.e.*,

$$X := \{x_K(u) \mid u \in [N]\} = \text{MPNN}_\theta(G), \quad X' := \{x'_K(u') \mid u' \in [N']\} = \text{MPNN}_\theta(G'). \quad (16)$$

243 The optimal alignment S is highly sensitive to the global structure of the graph pairs, *i.e.*, $S[e, e']$
 244 can significantly change when we perturb G or G' in regimes distant from e or e' . Conventional
 245 representations mitigate this sensitivity while training models, by setting non-edges to zero, rendering
 246 them invariant to structural changes. To address this limitation, we utilize more expressive graph
 247 representations, where non-edges are also embedded using trainable non-zero vectors. This approach
 248 allows information to be captured from the structure around the nodes through both edges and

249 non-edges, thereby enhancing the representational capacity of the embedding network. For each
 250 node-pair $e = (u, v) \in G$ (and equivalently (v, u)), and $e' = (u', v') \in G'$, the embeddings of the
 251 corresponding nodes and their connectivity status are concatenated, and then passed through an MLP
 252 to obtain the embedding vectors $r(e), r'(e') \in \mathbb{R}^D$. For $e = (u, v) \in G$, we compute $r(e)$ as follows:

$$r(e) = \text{MLP}_\theta(x_K(u) \parallel x_K(v) \parallel A[u, v]) + \text{MLP}_\theta(x_K(v) \parallel x_K(u) \parallel A[v, u]). \quad (17)$$

253 We can compute $r'(e)$ in similar manner. The property $r((u, v)) = r((v, u))$ reflects the undirected
 254 property of graph. Finally, the vectors $r(e)$ and $r'(e')$ are stacked into matrices R and R' , both with
 255 dimensions $\mathbb{R}^{\binom{N}{2} \times D}$. We would like to highlight that $r((u, v))$ or $r'((u', v'))$ are computed only
 256 once for all node-pairs, after the MPNN completes its final K th layer of execution. The message
 257 passing in the MPNN occurs only over edges. Therefore, this approach does not significantly increase
 258 the time complexity.

259 **Neural architecture of PERMNET $_\phi$** The network PERMNET $_\phi$ provides P as a soft node alignment
 260 matrix by taking the node embeddings as input, *i.e.*, $P = \text{PERMNET}_\phi(X, X')$. PERMNET $_\phi$ is
 261 implemented in two steps. In the first step, we apply a neural network c_ϕ on both x_K and x'_K ,
 262 and then compute the normed difference between their outputs to construct the matrix C , where
 263 $C[u, u'] = \|c_\phi(x_K(u)) - c_\phi(x'_K(u'))\|_1$. Next, we apply iterative Sinkhorn normalizations [16, 35]
 264 on $\exp(-C/\tau)$, to obtain a soft node alignment P . Therefore,

$$P = \text{Sinkhorn} \left(\left[\exp(-\|c_\phi(x_K(u)) - c_\phi(x'_K(u'))\|_1 / \tau) \right]_{(u, u') \in [N] \times [N]} \right). \quad (18)$$

265 Here, τ is a temperature hyperparameter. In a general cost setting, GED is typically asymmetric,
 266 so it may be desirable for $C[u, u']$ to be asymmetric with respect to x and x' . However, as noted
 267 in Proposition 1, when we compute GED(G', G), the alignment matrix $P' = \text{PERMNET}_\phi(X', X)$
 268 should satisfy the condition that $P' = P^\top$, where P is computed from Eq. (18). The current form of
 269 C supports this condition, whereas an asymmetric form might not, as shown in Appendix D.

270 We construct $S \in \mathbb{R}^{\binom{N}{2}} \times \mathbb{R}^{\binom{N}{2}}$ as follows. Each pair of nodes (u, v) in G and (u', v') in G' can
 271 be mapped in two ways, regardless of whether they are edges or non-edges: (1) node $u \mapsto u'$ and
 272 $v \mapsto v'$ which is denoted by $P[u, u']P[v, v']$; (2) node $u \mapsto v'$ and $v \mapsto u'$, which is denoted
 273 by $P[u, v']P[v, u']$. Combining these two scenarios, we compute the node-pair alignment matrix S
 274 as: $S[(u, v), (u', v')] = P[u, u']P[v, v'] + P[u, v']P[v, u']$. This explicit formulation of S from P
 275 ensures mutually consistent permutation across nodes and node-pairs.

276 4 Experiments

277 We conduct extensive experiments on GRAPHEDX to showcase the effectiveness of our method
 278 across several real-world datasets, under both equal and unequal cost settings for GED. Additional
 279 experimental results can be found in Appendix F.

280 4.1 Setup

281 **Datasets** We experiment with seven real-world datasets: Mutagenicity (Mutag) [18], Ogbg-Code2
 282 (Code2) [23], Ogbg-Molhiv (Molhiv) [23], Ogbg-Molpcba (Molpcba) [23], AIDS [36], Linux [5] and
 283 Yeast [36]. For each dataset’s training, test and validation sets $\mathcal{D}_{\text{split}}$, we generate $\binom{|\mathcal{D}_{\text{split}}|}{2} + |\mathcal{D}_{\text{split}}|$
 284 graph pairs, considering combinations between every two graphs, including self-pairing. We calculate
 285 the exact ground truth GED using the F2 solver [29], implemented within GEDLIB [10]. For GED
 286 with equal cost setting, we set the cost values to $b^\ominus = b^\oplus = a^\ominus = a^\oplus = 1$. For GED with unequal
 287 cost setting, we use $b^\ominus = 3, b^\oplus = 1, a^\ominus = 2, a^\oplus = 1$. Further details on dataset generation and
 288 statistics are presented in Appendix E. In the main paper, we present results for the first five datasets
 289 under both equal and unequal cost settings for GED. Additional experiments for Linux and Yeast, as
 290 well as GED with node label substitutions, are presented in Appendix F.

291 **Baselines** We compare our approach with nine state-of-the-art methods. These include two variants
 292 of GMN [31]: (1) GMN-Match and (2) GMN-Embed; (3) ISONET [43], (4) GREED [40], (5)
 293 ERIC [55], (6) SimGNN [5], (7) H2MN [53], (8) GraphSim [6] and (9) EGSC [39]. To compute
 294 the GED, GMN-Match, GMN-Embed, and GREED use the Euclidean distance between the vector
 295 representation of two graphs. ISONET uses an asymmetric distance specifically tailored to subgraph
 296 isomorphism. H2MN is an early interaction network that utilizes higher-order node similarity through
 297 hypergraphs. ERIC, SimGNN, and EGSC leverage neural networks to calculate the distance between two
 298 graphs. Furthermore, the last three methods predict a score based on the normalized GED in the

	GED with equal cost					GED with unequal cost				
	Mutag	Code2	Molhiv	Molpcba	AIDS	Mutag	Code2	Molhiv	Molpcba	AIDS
GMN-Match [31]	0.797	1.677	1.318	1.073	0.821	69.210	13.472	76.923	23.985	31.522
GMN-Embed [31]	1.032	1.358	1.859	1.951	1.044	72.495	13.425	78.254	28.437	33.221
ISONET [43]	1.187	0.879	1.354	1.106	1.640	3.369	3.025	3.451	2.781	5.513
GREED [40]	1.398	1.869	1.708	1.550	1.004	68.732	11.095	78.300	26.057	34.354
ERIC [55]	0.719	1.363	1.165	0.862	0.731	1.981	12.767	3.377	2.057	1.581
SimGNN [5]	1.471	2.667	1.609	1.456	1.455	4.747	5.212	4.145	3.465	4.316
H2MN [53]	1.278	7.240	1.521	1.402	1.114	3.413	9.435	3.782	3.396	3.105
GraphSim [6]	2.005	3.139	2.577	1.656	1.936	5.370	7.405	6.643	3.928	5.266
EGSC [39]	0.765	4.165	1.138	0.938	0.627	1.758	3.957	2.371	2.133	1.693
GRAPHEDX	0.492	0.429	0.781	0.764	0.565	1.134	1.478	1.804	1.677	1.252

Table 2: Prediction error measured in terms of MSE of GRAPHEDX and all the state-of-the-art baselines across five datasets on 20% test set, for GED with equal costs and unequal costs. For GED with equal (unequal) costs we have $b^\ominus = b^\oplus = a^\ominus = a^\oplus = 1$ ($b^\ominus = 3, b^\oplus = 1, a^\ominus = 2, a^\oplus = 1$.) We select $\Delta^\ominus(R, R' | S)$, $\Delta^\oplus(R, R' | S)$ and $\Delta^\ominus(X, X' | P)$, $\Delta^\oplus(X, X' | P)$ from the cartesian space of Edge- $\{\text{AlignDiff}, \text{DiffAlign}, \text{XOR-DiffAlign}\} \times \text{Node-}\{\text{AlignDiff}, \text{DiffAlign}, \text{XOR-DiffAlign}\}$ through cross validation. **Green** (**yellow**) numbers report the best (second best) performers.

form of $\exp(-2\text{GED}(G, G')/(|V| + |V'|))$. Notably, none of these baseline approaches have been designed to incorporate unequal edit costs into their models. To address this limitation, when working with GED under unequal cost setting, we include the edit costs as initial features in the graphs for all baseline models.

Evaluation Given a dataset $\mathcal{D} = \{(G_i, G'_i, \text{GED}(G_i, G'_i))\}_{i \in [n]}$, we divide it into training, validation and test folds with a split ratio of 60:20:20. We train the models using the Mean Squared Error (MSE) between the predicted GED and the ground truth GED as the loss. For model evaluation, we calculate the Mean Squared Error (MSE) between the actual and predicted GED on the test set. For ERIC, SimGNN and EGSC, we rescale the predicted score to obtain the true (unscaled) GED as $\text{GED}(G, G') = -(|V| + |V'|) \log(s)/2$. In Appendix F, we also report Kendall’s Tau (Ktau) to evaluate the rank correlation across different experiments.

Selection of $\Delta^\bullet(X, X' | P)$ and $\Delta^\bullet(R, R' | S)$ We have three neural distance surrogates to choose from — AlignDiff, DiffAlign and XOR-DiffAlign — for both edge and node edits, resulting in nine possible combinations. We experiment with each of these nine combinations and select the one with the lowest validation error. However, as we will see later, the best performing surrogates always incorporate XOR-DiffAlign for edge edits. Consequently, one can limit the cross validation to only three surrogates for node edits, while using XOR-DiffAlign as the fixed surrogate for edge edits.

4.2 Results

Comparison with baselines We start by comparing the performance of GRAPHEDX against all state-of-the-art baselines for GED with both equal and unequal costs. Table 2 summarizes the results. We make the following observations. (1) GRAPHEDX outperforms all the baselines by a significant margin. For GED with equal costs, this margin often goes as high as 15%. This advantage becomes even more pronounced for GED with unequal costs, where our method outperforms the baselines by a margin as high as 30%, as seen in Code2. (2) There is no clear second-best method. Among the baselines, EGSC and ERIC each outperforms the others in two out of five datasets for both equal and unequal cost settings. Also, EGSC demonstrates competitive performance in AIDS.

Impact of cost-guided GED Among the baselines, GMN-Match, GMN-Embed and GREED compute GED using the euclidean distance between the graph embeddings, *i.e.*, $\text{GED}(G, G') = \|x_G - x_{G'}\|_2$, whereas we compute it by summing the set distance surrogates between the node and edge embedding sets. To understand the impact of our cost guided distance, we adapt it to the graph-level embeddings used by the above three baselines as follows: $\text{GED}(G, G') = \frac{b^\ominus + a^\ominus}{2} \|\text{ReLU}(x_G - x_{G'})\|_1 + \frac{b^\oplus + a^\oplus}{2} \|\text{ReLU}(x_{G'} - x_G)\|_1$. Table 3 summarizes the results in terms of MSE, which shows that (1) cost guided distance reduces the MSE by a significant margin in most cases; (2) even in the setting of GED with equal costs, our set divergence formulation is a better surrogate compared to the baselines (3) the margin of improvement is more prominent with GED involving unequal costs, where the modeling of specific cost values is crucial (4) GRAPHEDX outperforms the baselines even after changing their default distance to our cost guided distance.

Benefits of all node-pairs representation In this section, we compare the performance of using graph representation with two variants of our method. (i) Edge-only (edge \rightarrow edge): Here, R, R'

	Equal cost			Unequal cost		
	Mutag	Code2	Molhiv	Mutag	Code2	Molhiv
GMN-Match	0.797	1.677	1.318	69.210	13.472	76.923
GMN-Match *	0.654	0.960	1.008	1.592	2.906	2.162
GMN-Embed	1.032	1.358	1.859	72.495	13.425	78.254
GMN-Embed *	1.011	1.179	1.409	2.368	3.272	3.413
GREED	1.398	1.869	1.708	68.732	11.095	78.300
GREED *	2.133	1.850	1.644	2.456	5.429	3.827
GRAPHEDX	0.492	0.429	0.781	1.134	1.478	1.804

Table 3: Impact of cost guided distance in terms of MSE; * represents the variant of the baseline with cost-guided distance. **Green (bold)** shows the best among all methods (only baselines).

338 $\in \mathbb{R}^{\max(|E|, |E'|) \times D}$ are computed using only the embeddings of node-pairs that are edges, and
339 excluding non-edges. This means that S becomes an edge-to-edge alignment matrix instead of a
340 full node-pair alignment matrix. (ii) Edge-only (pair \rightarrow pair): In this variant, S remains a node-pair
341 alignment matrix, but the embeddings of the non-edges in $R, R' \in \mathbb{R}^{N(N-1)/2 \times D}$ are explicitly set
342 to zero. In Table 4, we report the results in terms of MSE, which show that (1) both these sparse
343 representations perform significantly worse compared to our method using non-trivial representations
344 for both edges and non-edges, and (2) Edge-only (edge \rightarrow edge) performs better than Edge-only
345 (pair \rightarrow pair). This underscores the importance of explicitly modeling trainable non-edge embeddings
346 to capture the sensitivity of GED to global graph structure.

347 **Comparison across nine distances** Here, we compare among the nine different combinations of our
348 neural distance surrogates. Table 5 shows that the best combination mostly share the XOR-DiffAlign
349 on the edge edit. This is because, XOR-DiffAlign offers more inductive bias, by zeroing the edit cost
350 of aligning an edge to edge and a non-edge to non-edge, as we discussed in Section 3.2. There is no
winner between AlignDiff and DiffAlign.

Edge edit	Node edit	Equal cost		Unequal cost	
		Mutag	Code2	Mutag	Code2
DiffAlign	DiffAlign	0.579	0.740	1.205	2.451
DiffAlign	AlignDiff	0.557	0.742	1.211	2.116
DiffAlign	XOR	0.538	0.719	1.146	1.896
AlignDiff	DiffAlign	0.537	0.513	1.185	1.689
AlignDiff	AlignDiff	0.578	0.929	1.338	1.488
AlignDiff	XOR	0.533	0.826	1.196	1.741
XOR	AlignDiff	0.492	0.429	1.134	1.478
XOR	DiffAlign	0.510	0.634	1.148	1.489
XOR	XOR	0.530	1.588	1.195	2.507

Table 5: Comparison among the nine neural distance combinations. **Green (yellow)** indicate the best (second best) performers in terms of MSE.

351

352 **Performance for GED under node substitution cost** The scoring function in Eq. 9 can also be
353 extended to incorporate node label substitution cost, which has been described in Appendix D. Here,
354 we compare the performance of our model with the baselines in terms of MSE where we include
355 node substitution cost b^\sim , with cost setting as $b^\ominus = b^\oplus = b^\sim = a^\ominus = a^\oplus = 1$. In Table 6, we report
356 the results across 5 datasets equipped with node labels, passed as one-hot encoded node features. We
357 observe that (1) our model outperforms all other baselines across all datasets by significant margin;
358 (2) there is no clear second winner but ERIC, EGSC and ISONET performs better than the others.

359 5 Conclusion

360 Our work introduces a novel neural model for computing GED that explicitly incorporates general
361 costs of edit operations. By leveraging graph representations that recognize both edges and non-edges,
362 together with the design of suitable set distance surrogates, we achieve a more robust neural surrogate
363 for GED. Our experiments demonstrate that this approach outperforms state-of-the-art methods,
364 especially in settings with general edit costs, providing a flexible and effective solution for a range
365 of applications. A potential limitation is that real-world applications often involve richly attributed
366 graphs, where relevance based on GED might require separate formulations for modeling the structure
367 of edit operations and the similarity of all node-pair features. Future work could focus on developing
368 specialized formulations that integrate domain-specific knowledge, that improve effectiveness of
369 GED-based graph comparison across various domains.

	Equal cost			Unequal cost		
	Mutag	Code2	Molhiv	Mutag	Code2	Molhiv
Edge-only (edge \rightarrow edge)	0.566	0.683	0.858	1.274	1.817	1.847
Edge-only (pair \rightarrow pair)	0.596	0.760	0.862	1.276	1.879	1.865
GRAPHEDX	0.492	0.429	0.781	1.134	1.478	1.804

Table 4: Benefits of all node-pair representation MSE using only edges vs. all node-pair representations. **Green (yellow)** indicate the best (second best) performers.

	Mutag	Code2	Molhiv	Molpcba	AIDS
GMN-Match	1.057	5.224	1.388	1.432	0.868
GMN-Embed	2.159	4.070	3.523	4.657	1.818
ISONET	0.876	1.129	1.617	1.332	1.142
GREED	2.876	4.983	2.923	3.902	2.175
ERIC	0.886	6.323	1.537	1.278	1.602
SimGNN	1.160	5.909	1.888	2.172	1.418
H2MN	1.277	6.783	1.891	1.666	1.290
GraphSim	1.043	4.708	1.817	1.748	1.561
EGSC	0.776	8.742	1.273	1.426	1.270
GRAPHEDX	0.441	0.820	0.792	0.846	0.538

Table 6: MSE for different methods with unit node substitution cost in equal cost setting. **Green (yellow)** show (second) best method.

References

- 370
371 [1] J. Adler and S. Lutz. Banach wasserstein gan. *Advances in neural information processing*
372 *systems*, 31, 2018.
- 373 [2] B. Amos, L. Xu, and J. Z. Kolter. Input convex neural networks. In *International Conference*
374 *on Machine Learning*, pages 146–155. PMLR, 2017.
- 375 [3] M. Arjovsky, S. Chintala, and L. Bottou. Wasserstein generative adversarial networks. In
376 *International conference on machine learning*, pages 214–223. PMLR, 2017.
- 377 [4] A. Backurs, Y. Dong, P. Indyk, I. Razenshteyn, and T. Wagner. Scalable nearest neighbor search
378 for optimal transport. In *International Conference on machine learning*, pages 497–506. PMLR,
379 2020.
- 380 [5] Y. Bai, H. Ding, S. Bian, T. Chen, Y. Sun, and W. Wang. Simgnn: A neural network approach to
381 fast graph similarity computation. In *Proceedings of the Twelfth ACM International Conference*
382 *on Web Search and Data Mining*, pages 384–392, 2019.
- 383 [6] Y. Bai, H. Ding, K. Gu, Y. Sun, and W. Wang. Learning-based efficient graph similarity
384 computation via multi-scale convolutional set matching. In *Proceedings of the AAAI Conference*
385 *on Artificial Intelligence*, volume 34, pages 3219–3226, 2020.
- 386 [7] D. B. Blumenthal. New techniques for graph edit distance computation. *arXiv preprint*
387 *arXiv:1908.00265*, 2019.
- 388 [8] D. B. Blumenthal and J. Gamper. Improved lower bounds for graph edit distance. *IEEE*
389 *Transactions on Knowledge and Data Engineering*, 30:503–516, 2018. URL [https://api.
390 semanticscholar.org/CorpusID:3438059](https://api.semanticscholar.org/CorpusID:3438059).
- 391 [9] D. B. Blumenthal, E. Daller, S. Bogleux, L. Brun, and J. Gamper. Quasimetric graph edit
392 distance as a compact quadratic assignment problem. In *2018 24th International Conference on*
393 *Pattern Recognition (ICPR)*, pages 934–939, 2018. doi: 10.1109/ICPR.2018.8546055.
- 394 [10] D. B. Blumenthal, S. Bogleux, J. Gamper, and L. Brun. Gedlib: A c++ library for graph
395 edit distance computation. In D. Conte, J.-Y. Ramel, and P. Foggia, editors, *Graph-Based*
396 *Representations in Pattern Recognition*, pages 14–24, Cham, 2019. Springer International
397 Publishing. ISBN 978-3-030-20081-7.
- 398 [11] S. Bogleux, L. Brun, V. Carletti, P. Foggia, B. Gaüzère, and M. Vento. Graph edit distance as a
399 quadratic assignment problem. *Pattern Recognition Letters*, 87:38–46, 2017. ISSN 0167-8655.
400 doi: <https://doi.org/10.1016/j.patrec.2016.10.001>. URL [https://www.sciencedirect.com/
401 science/article/pii/S0167865516302665](https://www.sciencedirect.com/science/article/pii/S0167865516302665). Advances in Graph-based Pattern Recognition.
402 tion.
- 403 [12] A. Z. Broder, M. Charikar, A. M. Frieze, and M. Mitzenmacher. Min-wise independent
404 permutations. In *Proceedings of the thirtieth annual ACM symposium on Theory of computing*,
405 pages 327–336, 1998.
- 406 [13] H. Bunke. On a relation between graph edit distance and maximum common subgraph. *Pattern*
407 *Recognition Letters*, 18(8):689–694, 1997.
- 408 [14] H. Bunke and G. Allermann. Inexact graph matching for structural pattern recognition. *Pattern*
409 *Recognition Letters*, 1(4):245–253, 1983.
- 410 [15] L. Chang, X. Feng, X. Lin, L. Qin, and W. Zhang. Efficient graph edit distance computation and
411 verification via anchor-aware lower bound estimation. *arXiv preprint arXiv:1709.06810*, 2017.
- 412 [16] M. Cuturi. Sinkhorn distances: Lightspeed computation of optimal transport. *Advances in*
413 *neural information processing systems*, 26:2292–2300, 2013.
- 414 [17] M. Daniels, T. Maunu, and P. Hand. Score-based generative neural networks for large-scale
415 optimal transport. *Advances in neural information processing systems*, 34:12955–12965, 2021.

- 416 [18] A. K. Debnath, R. L. Lopez de Compadre, G. Debnath, A. J. Shusterman, and C. Hansch.
417 Structure-activity relationship of mutagenic aromatic and heteroaromatic nitro compounds.
418 correlation with molecular orbital energies and hydrophobicity. *Journal of Medicinal Chem-*
419 *istry*, 34(2):786–797, 1991. doi: 10.1021/jm00106a046. URL [https://doi.org/10.1021/
420 jm00106a046](https://doi.org/10.1021/jm00106a046).
- 421 [19] K. D. Doan, S. Manchanda, S. Mahapatra, and C. K. Reddy. Interpretable graph similarity
422 computation via differentiable optimal alignment of node embeddings. In *Proceedings of
423 the 44th International ACM SIGIR Conference on Research and Development in Information
424 Retrieval*, pages 665–674, 2021.
- 425 [20] M. Douze, A. Guzhva, C. Deng, J. Johnson, G. Szilvassy, P.-E. Mazaré, M. Lomeli, L. Hosseini,
426 and H. Jégou. The faiss library. *arXiv preprint arXiv:2401.08281*, 2024.
- 427 [21] C. Garcia-Hernandez, A. Fernandez, and F. Serratos. Ligand-based virtual screening using
428 graph edit distance as molecular similarity measure. *Journal of chemical information and
429 modeling*, 59(4):1410–1421, 2019.
- 430 [22] A. Genevay, M. Cuturi, G. Peyré, and F. Bach. Stochastic optimization for large-scale optimal
431 transport. *Advances in neural information processing systems*, 29, 2016.
- 432 [23] W. Hu, M. Fey, M. Zitnik, Y. Dong, H. Ren, B. Liu, M. Catasta, and J. Leskovec. Open
433 graph benchmark: Datasets for machine learning on graphs. *Advances in neural information
434 processing systems*, 33:22118–22133, 2020.
- 435 [24] P. Indyk and R. Motwani. Approximate nearest neighbors: towards removing the curse of
436 dimensionality. In *Proceedings of the thirtieth annual ACM symposium on Theory of computing*,
437 pages 604–613, 1998.
- 438 [25] P. Indyk, R. Motwani, P. Raghavan, and S. Vempala. Locality-preserving hashing in multidimensional
439 spaces. In *Proceedings of the twenty-ninth annual ACM symposium on Theory of
440 computing*, pages 618–625, 1997.
- 441 [26] S. Ivanov, S. Sviridov, and E. Burnaev. Understanding isomorphism bias in graph data sets.
442 arXiv 1910.12091, 2019. URL <https://arxiv.org/abs/1910.12091>.
- 443 [27] D. Justice and A. Hero. A binary linear programming formulation of the graph edit distance.
444 *IEEE Transactions on Pattern Analysis and Machine Intelligence*, 28(8):1200–1214, 2006.
- 445 [28] M. G. Kendall. A new measure of rank correlation. *Biometrika*, 30(1/2):81–93, 1938.
- 446 [29] J. Lerouge, Z. Abu-Aisheh, R. Raveaux, P. Héroux, and S. Adam. New binary linear pro-
447 gramming formulation to compute the graph edit distance. *Pattern Recognition*, 72:254–
448 265, 2017. ISSN 0031-3203. doi: <https://doi.org/10.1016/j.patcog.2017.07.029>. URL
449 <https://www.sciencedirect.com/science/article/pii/S003132031730300X>.
- 450 [30] Y. Li, D. Tarlow, M. Brockschmidt, and R. Zemel. Gated graph sequence neural networks.
451 *arXiv preprint arXiv:1511.05493*, 2015.
- 452 [31] Y. Li, C. Gu, T. Dullien, O. Vinyals, and P. Kohli. Graph matching networks for learning the
453 similarity of graph structured objects. In *International conference on machine learning*, pages
454 3835–3845. PMLR, 2019.
- 455 [32] C.-L. Lin. Hardness of approximating graph transformation problem. In D.-Z. Du and X.-S.
456 Zhang, editors, *Algorithms and Computation*, pages 74–82, Berlin, Heidelberg, 1994. Springer
457 Berlin Heidelberg. ISBN 978-3-540-48653-4.
- 458 [33] Z. Lou, J. You, C. Wen, A. Canedo, J. Leskovec, et al. Neural subgraph matching. *arXiv
459 preprint arXiv:2007.03092*, 2020.
- 460 [34] Y. A. Malkov and D. A. Yashunin. Efficient and robust approximate nearest neighbor search
461 using hierarchical navigable small world graphs. *IEEE transactions on pattern analysis and
462 machine intelligence*, 42(4):824–836, 2018.

- 463 [35] G. Mena, D. Belanger, S. Linderman, and J. Snoek. Learning latent permutations with gumbel-
464 sinkhorn networks. *arXiv preprint arXiv:1802.08665*, 2018. URL [https://arxiv.org/pdf/
465 1802.08665.pdf](https://arxiv.org/pdf/1802.08665.pdf).
- 466 [36] C. Morris, N. M. Kriege, F. Bause, K. Kersting, P. Mutzel, and M. Neumann. Tudataset: A
467 collection of benchmark datasets for learning with graphs, 2020.
- 468 [37] B. Naidan, L. Boytsov, Y. Malkov, and D. Novak. Non-metric space library manual. *arXiv
469 preprint arXiv:1508.05470*, 2015.
- 470 [38] E. Ozdemir and C. Gunduz-Demir. A hybrid classification model for digital pathology using
471 structural and statistical pattern recognition. *IEEE Transactions on Medical Imaging*, 32(2):
472 474–483, 2013. doi: 10.1109/TMI.2012.2230186.
- 473 [39] C. Qin, H. Zhao, L. Wang, H. Wang, Y. Zhang, and Y. Fu. Slow learning and fast inference:
474 Efficient graph similarity computation via knowledge distillation. In *Thirty-Fifth Conference on
475 Neural Information Processing Systems*, 2021.
- 476 [40] R. Ranjan, S. Grover, S. Medya, V. Chakaravarthy, Y. Sabharwal, and S. Ranu. Greed: A neural
477 framework for learning graph distance functions. *Advances in Neural Information Processing
478 Systems*, 35:22518–22530, 2022.
- 479 [41] K. Riesen and H. Bunke. Approximate graph edit distance computation by means of bipartite
480 graph matching. *Image and Vision Computing*, 27(7):950–959, 2009. ISSN 0262-8856.
481 doi: <https://doi.org/10.1016/j.imavis.2008.04.004>. URL [https://www.sciencedirect.com/
482 science/article/pii/S026288560800084X](https://www.sciencedirect.com/science/article/pii/S026288560800084X). 7th IAPR-TC15 Workshop on Graph-based
483 Representations (GbR 2007).
- 484 [42] K. Riesen, A. Fischer, and H. Bunke. Combining bipartite graph matching and beam search for
485 graph edit distance approximation. In *Artificial Neural Networks in Pattern Recognition: 6th
486 IAPR TC 3 International Workshop, ANNPR 2014, Montreal, QC, Canada, October 6-8, 2014.
487 Proceedings 6*, pages 117–128. Springer, 2014.
- 488 [43] I. Roy, V. S. Velugoti, S. Chakrabarti, and A. De. Interpretable neural subgraph matching for
489 graph retrieval. *AAAI*, 2022.
- 490 [44] S. Sahni and T. Gonzalez. P-complete approximation problems. *J. ACM*, 23(3):555–565, jul
491 1976. ISSN 0004-5411. doi: 10.1145/321958.321975. URL [https://doi.org/10.1145/
492 321958.321975](https://doi.org/10.1145/321958.321975).
- 493 [45] A. Sanfeliu and K.-S. Fu. A distance measure between attributed relational graphs for pattern
494 recognition. *IEEE transactions on systems, man, and cybernetics*, pages 353–362, 1983.
- 495 [46] A. Sanfeliu, R. Alquézar, J. Andrade, J. Climent, F. Serratos, and J. Vergés. Graph-based
496 representations and techniques for image processing and image analysis. *Pattern recognition*,
497 35(3):639–650, 2002.
- 498 [47] V. Seguy, B. B. Damodaran, R. Flamary, N. Courty, A. Rolet, and M. Blondel. Large-scale
499 optimal transport and mapping estimation. *arXiv preprint arXiv:1711.02283*, 2017.
- 500 [48] K. Shearer, H. Bunke, and S. Venkatesh. Video indexing and similarity retrieval by largest
501 common subgraph detection using decision trees. *Pattern Recognition*, 34(5):1075–1091, 2001.
- 502 [49] R. Sinkhorn and P. Knopp. Concerning nonnegative matrices and doubly stochastic matrices.
503 *Pacific Journal of Mathematics*, 21(2):343–348, 1967.
- 504 [50] S. Tirthapura, D. Sharvit, P. Klein, and B. B. Kimia. Indexing based on edit-distance matching
505 of shape graphs. In *Multimedia storage and archiving systems III*, volume 3527, pages 25–36.
506 SPIE, 1998.
- 507 [51] Y. Xie, M. Chen, H. Jiang, T. Zhao, and H. Zha. On scalable and efficient computation of large
508 scale optimal transport. In *International Conference on Machine Learning*, pages 6882–6892.
509 PMLR, 2019.

- 510 [52] Z. Zeng, A. K. Tung, J. Wang, J. Feng, and L. Zhou. Comparing stars: On approximating graph
511 edit distance. *Proceedings of the VLDB Endowment*, 2(1):25–36, 2009.
- 512 [53] Z. Zhang, J. Bu, M. Ester, Z. Li, C. Yao, Z. Yu, and C. Wang. H2mn: Graph similarity
513 learning with hierarchical hypergraph matching networks. In *Proceedings of the 27th ACM*
514 *SIGKDD Conference on Knowledge Discovery & Data Mining*, KDD '21, page 2274–2284,
515 New York, NY, USA, 2021. Association for Computing Machinery. ISBN 9781450383325. doi:
516 10.1145/3447548.3467328. URL <https://doi.org/10.1145/3447548.3467328>.
- 517 [54] W. Zheng, L. Zou, X. Lian, D. Wang, and D. Zhao. Efficient graph similarity search over large
518 graph databases. *IEEE Transactions on Knowledge and Data Engineering*, 27(4):964–978,
519 2014.
- 520 [55] W. Zhuo and G. Tan. Efficient graph similarity computation with alignment regularization.
521 *Advances in Neural Information Processing Systems*, 35:30181–30193, 2022.

522 **Graph Edit Distance with General Costs**
523 **Using Neural Set Divergence**
524 **(Appendix)**

525 **A Limitations**

526 Our neural model for GED affords significant improvements in accuracy and flexibility for modeling
527 edit costs. However, there are some limitations to consider.

528 (1) While computing graph representations over $\binom{N}{2} \times \binom{N}{2}$ node-pairs does not require additional
529 parameters due to parameter-sharing, it does demand significant memory resources. This could pose
530 challenges, especially with larger-sized graphs.

531 (2) The assumption of fixed edit costs across all graph pairs within a dataset might not reflect real-
532 world scenarios where costs vary based on domain-specific factors and subjective human relevance
533 judgements. This calls for more specialized approaches to accurately model the impact of each edit
534 operation, which may differ across node pairs.

535 (3) the current model may not adequately address richly attributed graphs with complex node and
536 edge features. Incorporating such attributes alongside graph structure based GED computation may
537 require further exploration.

538 **B Broader impact**

539 Graphs serve as powerful representations across diverse domains, capturing complex relationships
540 and structural notions inherent in various systems. From biological networks to social networks,
541 transportation networks, and supply chains, graphs provide a versatile framework for modeling
542 interactions between interconnected entities. In domains where structure-similarity based applications
543 are prevalent, GED emerges as a valuable and versatile tool.

544 For example, in bio-informatics, molecular structures can naturally be represented as graphs. GED
545 computation expedites tasks such as drug discovery, protein-protein interaction modeling, and
546 molecular similarity analysis by identifying structurally similar molecular compounds. Similarly,
547 in social network analysis, GED can measure similarities between user interactions, aiding in
548 friend recommendation systems or community detection tasks. In transportation networks, GED-
549 based tools assess similarity between road networks for route planning or traffic optimizations.
550 Further applications include learning to edit scene graphs, analyzing gene regulatory pathways, fraud
551 detection, and more

552 Moreover, our proposed variations of GED, particularly those amenable to hashing, find utility in
553 retrieval based setups. In various information retrieval systems, hashed graph representations can be
554 used to efficiently index and retrieve relevant items using our GED based scores. Such applications
555 include image retrieval from image databases where images are represented as scene graphs, retrieval
556 of relevant molecules from molecular databases, *etc.*

557 Furthermore, our ability to effectively model different edit costs in GED opens up new possibilities
558 in various applications. In recommendation systems, it can model user preferences of varying
559 importance, tailoring recommendations based on user-specific requirements or constraints. Similarly,
560 in image or video processing, different types of distortions may have varying impacts on perceptual
561 quality, and GED with adaptive costs can better assess similarity. In NLP tasks such as text similarity
562 understanding and document clustering, assigning variable costs to textual edits corresponding to
563 word insertion, deletions or substitutions, provides a more powerful framework for measuring textual
564 similarity, improving performance in downstream tasks such as plagiarism detection, summarization,
565 *etc.*

566 Lastly, and most importantly, the design of our model encourages interpretable alignment-driven
567 justifications, thereby promoting transparency and reliability while minimizing potential risks and
568 negative impacts, in high stake applications like drug discovery.

569 **C Discussion on related work**

570 **Heuristics for Graph Edit Distance** GED was first introduced in [45]. Bunke and Allermann
571 [14] used it as a tool for non exact graph matching. Later on, [13] connected GED with maximum
572 common subgraph estimation. Blumenthal [7] provide an excellent survey. As they suggest,
573 combinatorial heuristics to solve GED predominantly follows three approaches: (1) Linear sum
574 assignment problem with error-correction, which include [27, 41, 52, 54] (2) Linear programming,
575 which predominantly uses standard tools like Gurobi, (3) Local search [42]. However, they can be
576 extremely time consuming, especially for a large number of graph pairs. Among them Zheng et al.
577 [54] operate in our problem setting, where the cost of edits are different across the edit operations,
578 but for the same edit operation, the cost is same across node or node pairs.

579 **Optimal transport** In our work, we utilize Graph Neural Networks (GNNs) to represent each graph
580 as a set of node embeddings. This transforms the inherent Quadratic Assignment Problem (QAP)
581 of graph matching into a Linear Sum Assignment Problem (LSAP) on the sets of node embeddings.
582 Essentially, this requires solving an optimal transport problem in the node embedding space. The use
583 of neural surrogates for optimal transport was first proposed by Cuturi [16], who introduced entropy
584 regularization to make the optimal transport objective strictly convex and utilized Sinkhorn iterations
585 [49] to obtain the transport plan. Subsequently, Mena et al. [35] proposed the neural Gumbel Sinkhorn
586 network as a continuous and differentiable surrogate of a permutation matrix, which we incorporate
587 into our model.

588 In various generative modeling applications, optimal transport costs are used as loss functions, such
589 as in Wasserstein GANs [1, 3]. Computing the optimal transport plan is a significant challenge,
590 with approaches leveraging the primal formulation [51, 33], the dual formulation with entropy
591 regularization [17, 47, 22], or Input Convex Neural Networks (ICNNs) [2].

592 **Neural graph similarity computation** Most earlier works on neural graph similarity computation
593 have focused on training with GED values as ground truth [5, 6, 19, 40, 55, 39, 53, 31], while some
594 have used MCS as the similarity measure [6, 5]. Current neural models for GED approximation
595 primarily follow two approaches. The first approach uses a trainable nonlinear function applied to
596 graph embeddings to compute GED [5, 39, 6, 55, 53, 19]. The second approach calculates GED
597 based on the Euclidean distance in the embedding space [31, 40].

598 Among these models, GOTSIM [19] focuses solely on node insertion and deletion, and computes
599 node alignment using a combinatorial routine that is decoupled from end-to-end training. However,
600 their network struggles with training efficiency due to the operations on discrete values, which
601 are not amenable to backpropagation. With the exception of GREED [40] and Graph Embedding
602 Network (GEN) [31], most methods use early interaction or nonlinear scoring functions, limiting
603 their adaptability to efficient indexing and retrieval pipelines

604 D Discussion on our proposed formulation of GED

605 D.1 Modification of scoring function from label substitution

606 To incorporate the effect of node substitution into account when formulating the GED, we first
 607 observe that the effect of node substitution cost b^\sim only comes into account when a non-padded
 608 node maps to a non-padded node. In all other cases, when a node is deleted or inserted, we do not
 609 additionally incur any substitution costs. Note that, we consider the case when node substitution
 610 cannot be replaced by node addition and deletion, *i.e.*, $b^\sim \leq b^\ominus + b^\oplus$. Such a constraint on costs
 611 has uses in multiple applications [9, 38]. Let \mathcal{L} denote the set of node labels, and $\ell(u), \ell'(u') \in \mathcal{L}$
 612 denote the node label corresponding to nodes u and u' in G and G' respectively. We construct the
 613 node label matrix L for G as follows: $L \in \{0, 1\}^{N \times |\mathcal{L}|}$, such that $L[i, :] = \text{one_hot}(\ell(i))$, *i.e.*, L is
 614 the one-hot indicator matrix for the node labels, which each row corresponding to the one-hot vector
 615 of the label. Similarly, we can construct L' for G' . Then, the distance between labels of two nodes
 616 $u \in V$ and $u' \in V'$ can be given as $\|L[u, :] - L'[u', :]\|_1$. To ensure that only valid node to node
 617 mappings contribute to the cost, we multiply the above with $\Lambda(u, u') = \text{AND}(\eta_G[u], \eta_{G'}[u'])$. This
 618 allows us to write the expression for GED with node label substitution cost as

$$\begin{aligned} \text{GED}(G, G') = \min_{P \in \mathbb{P}_N} & \frac{a^\ominus}{2} \|\text{ReLU}(A - PA'P^\top)\|_{1,1} + \frac{a^\oplus}{2} \|\text{ReLU}(PA'P^\top - A)\|_{1,1} \\ & + b^\ominus \|\text{ReLU}(Pq_{G'} - q_G)\|_1 + b^\oplus \|\text{ReLU}(q_G - Pq_{G'})\|_1 \\ & + b^\sim \underbrace{\sum_{u, u'} \Lambda(u, u') \|L[u, :] - L'[u', :]\|_1 P[u, u']}_{\Delta^\sim(L, L'|P)} \end{aligned}$$

619 We can design a neural surrogate for above in the same way as done in Section 3.2, and write

$$\begin{aligned} \text{GED}_{\theta, \phi}(G, G') = & a^\ominus \Delta^\ominus(R, R' | S) + a^\oplus \Delta^\oplus(R, R' | S) \\ & + b^\ominus \Delta^\ominus(X, X' | P) + b^\oplus \Delta^\oplus(X, X' | P) \\ & + b^\sim \Delta^\sim(L, L' | P) \end{aligned} \quad (19)$$

620 In this case, to account for node substitutions in the proposed permutation, we use $L[u, :]$ and $L'[u', :]$
 621 as the features for node u in G and node u' in G' , respectively. We present the comparison of our
 622 method including substitution cost with state-of-the-art baselines in Appendix F.

623 D.2 Proof of Proposition 1

624 **Proposition** Given a fixed set of values of $b^\ominus, b^\oplus, a^\ominus, a^\oplus$, let P be an optimal node permutation
 625 matrix corresponding to $\text{GED}(G, G')$, computed using Eq. (7). Then, $P' = P^\top$ is an optimal node
 626 permutation corresponding to $\text{GED}(G', G)$.

627 *Proof:* Noticing that $\text{ReLU}(c - d) = \max(c, d) - d$, we can write

$$\begin{aligned} \|\text{ReLU}(A - PA'P^\top)\|_{1,1} &= \|\max(A, PA'P^\top) - PA'P^\top\|_{1,1} \\ &= \|\max(A, PA'P^\top)\|_{1,1} - 2|E'| \end{aligned}$$

628 The last equality follows since $\max(A, PA'P^\top) \geq PA'P^\top$ element-wise, and $\|PA'P^\top\|_{1,1} =$
 629 $\|A'\|_{1,1} = 2|E'|$. Similarly, we can rewrite $\|\text{ReLU}(PA'P^\top - A)\|_{1,1}$, $\|\text{ReLU}(\eta_G - P\eta_{G'})\|_1$,
 630 and $\|\text{ReLU}(P\eta_{G'} - q_G)\|_1$, and finally rewrite Eq. (7) as

$$\begin{aligned} \text{GED}(G, G') = \min_{P \in \mathbb{P}_N} & \frac{a^\oplus + a^\ominus}{2} \|\max(A, PA'P^\top)\|_{1,1} - a^\ominus|E'| - a^\oplus|E| \\ & + \frac{b^\oplus + b^\ominus}{2} \|\max(\eta_G, P\eta_{G'})\|_1 - b^\ominus|V'| - b^\oplus|V| \end{aligned} \quad (20)$$

631

$$\begin{aligned} \text{GED}(G', G) = \min_{P \in \mathbb{P}_N} & \frac{a^\oplus + a^\ominus}{2} \|\max(A', PAP^\top)\|_{1,1} - a^\ominus|E| - a^\oplus|E'| \\ & + \frac{b^\oplus + b^\ominus}{2} \|\max(\eta_{G'}, P\eta_G)\|_1 - b^\ominus|V| - b^\oplus|V'| \end{aligned} \quad (21)$$

632

633 We can rewrite the max term as follows:

$$\begin{aligned}
\|\max(A, PA'P^\top)\|_{1,1} &= \sum_{u,v} \max(A, PA'P^\top)[u, v] \\
&= \sum_{u,v} \max(PP^\top APP^\top, PA'P^\top)[u, v] \\
&= \sum_{u,v} P \max(P^\top AP, A')P^\top[u, v] \\
&= \sum_{u,v} \max(P^\top AP, A')[u, v] \\
&= \|\max(P^\top AP, A')\|_{1,1} = \|\max(A', P^\top AP)\|_{1,1}
\end{aligned}$$

634 Similarly we can re write $\|\max(\eta_G, P\eta_{G'})\|_1$ as $\|\max(\eta_{G'}, P^\top \eta_G)\|_1$. Given a fixed set of cost
635 function $b^\ominus, b^\oplus, a^\ominus, a^\oplus$, the terms containing $|E'|, |E|, |V'|, |V|$ are constant and do not affect
636 choosing an optimal P . Let $C = -a^\ominus|E'| - a^\oplus|E| - b^\ominus|V| - b^\oplus|V'|$, Using the above equations,
637 we can write:

$$\begin{aligned}
&\frac{a^\oplus + a^\ominus}{2} \|\max(A, PA'P^\top)\|_{1,1} + \frac{b^\oplus + b^\ominus}{2} \|\max(\eta_G, P\eta_{G'})\|_1 \\
&= \frac{a^\oplus + a^\ominus}{2} \|\max(A', P^\top AP)\|_{1,1} + \frac{b^\oplus + b^\ominus}{2} \|\max(\eta_{G'}, P^\top \eta_G)\|_1
\end{aligned}$$

638 Let the first term be $\rho(G, G' | P)$. Then second term can be expressed as $\rho(G', G | P^\top)$ and
639 $\rho(G, G' | P) = \rho(G', G | P^\top)$ for all $P \in \mathbb{P}_N$. If P is the optimal solution of $\min_{P \in \mathbb{P}_N} \rho(G, G' | P)$
640 then, $\rho(G', G | P^\top) = \rho(G, G' | P) \leq \rho(G, G' | P'^\top) = \rho(G', G | \tilde{P})$ for any permutation \tilde{P} . Hence,
641 $P' = P^\top \in \mathbb{P}_N$ is one optimal solution.

642 D.3 Connections with other notions of graph matching

643 *Graph isomorphism:* When we set all costs to zero, we can write that $\text{GED}(G, G') =$
644 $\min_P 0.5 \|A - PA'P^\top\|_{1,1} + \|\eta_G - P\eta_{G'}\|_1$. In such a scenario, $\text{GED}(G, G')$ is symmetric, *i.e.*,
645 $\text{GED}(G', G) = \text{GED}(G, G')$ and it becomes zero only when G and G' are isomorphic.

646 *Subgraph isomorphism:* Assume $b^\ominus = b^\oplus = 0$. Then, if we set the cost of edge addition
647 to be arbitrarily small as compared to the cost of edge deletion, *i.e.*, $a^\oplus \ll a^\ominus$. This yields
648 $\text{GED}(G, G') = \min_P (b^\ominus \sum_{u,v} \text{ReLU}(A - PA'P^\top)[u, v])$, which can be reduced to zero for
649 some permutation $P, G \subseteq G'$.

650 *Maximum common edge subgraph:* From Appendix D.2, we can write that $\text{GED}(G, G') =$
651 $\min_P 0.5(a^\oplus + a^\ominus) \|\max(A, PA'P^\top)\|_{1,1} + (b^\oplus + b^\ominus) \|\eta_G, P\eta_{G'}\|_1 - a^\ominus|E'| - a^\oplus|E| - b^\ominus|V'| -$
652 $b^\oplus|V|$. When $a^\ominus = a^\oplus = 1$ and $b^\oplus = b^\ominus = 0$, then $\text{GED}(G, G') = \|\max(A, PA'P^\top)\|_{1,1} =$
653 $|E| + |E'| - \|\min(A, PA'P^\top)\|_{1,1}$. Here, $\min(A, PA'P^\top)$ characterizes maximum common edge
654 subgraph and $\|\min(A, PA'P^\top)\|_{1,1}$ provides the number of edges of it.

655 D.4 Relation between AlignDiff and DiffAlign

656 **Lemma 2** Let $Z, Z' \in \mathbb{R}^{N \times M}$, and $S \in \mathbb{R}_{\geq 0}^{N \times N}$ be double stochastic. Then,

$$\|\text{ReLU}(Z - SZ')\|_{1,1} \leq \sum_{i,j} \|\text{ReLU}(Z[i, :] - Z'[j, :])\|_1 S[i, j]$$

657 *Proof:* We can write,

$$\begin{aligned}
\|\text{ReLU}(Z - SZ')\|_{1,1} &= \sum_{i,j} \left| \text{ReLU} \left(Z[i,j] - \sum_k S[i,k]Z'[k,j] \right) \right| \\
&\stackrel{(*)}{=} \sum_{i,j} \text{ReLU} \left(\sum_k S[i,k]Z[i,j] - S[i,k]Z'[k,j] \right) \\
&\stackrel{(**)}{\leq} \sum_{i,j} \sum_k S[i,k] \text{ReLU}(Z[i,j] - Z'[k,j]) \\
&= \sum_{i,k} \|\text{ReLU}(Z[i,:] - Z'[k,:])\|_1 S[i,k] \quad \square
\end{aligned}$$

658 where $(*)$ follows since $\sum_k S[i,k] = 1 \forall i \in [N]$, and $(**)$ follows due to convexity of $\text{ReLU}(\cdot)$.
659 Now, notice that when $S \in \mathbb{P}_N$, then $S[i, \cdot]$ is 1 at one element while 0 at the rest. In that case, we
660 have

$$\begin{aligned}
\sum_{i,j} \text{ReLU} \left(\sum_k S[i,k]Z[i,j] - S[i,k]Z'[k,j] \right) &= \sum_{i,j} \text{ReLU}(Z[i,j] - Z'[k_i^*, j]) \\
&= \sum_{i,j} \sum_k S[i,k] \text{ReLU}(Z[i,j] - Z'[k,j])
\end{aligned}$$

661 where k_i^* is the index where $S[i, \cdot]$ is 1. Hence, we have an equality when S is a hard permutation.
662 Replacing (Z, Z') with (R, R') and (X, X') , we get that AlignDiff and DiffAlign are equivalent
663 when S is a hard permutation matrix, and moreover DiffAlign is an upper bound on AlignDiff when
664 S is a soft permutation matrix.

665 **D.5 Proof that our design ensures $P' = P^\top$**

666 Here we show why it is necessary to have a symmetric form for $C[u, u']$ in PERMNET_ϕ .
667 For $\text{GED}(G, G')$,

$$C[u, v] = \|c_\phi(x_K(u)) - c_\phi(x'_K(v))\|_1$$

668 For $\text{GED}(G', G)$,

$$C'[v, u] = \|c_\phi(x'_K(v)) - c_\phi(x_K(u))\|_1$$

669 Because the Sinkhorn cost $C[u, v]$ is symmetric, using the above equations we can infer,

$$\begin{aligned}
C[u, v] &= C'[v, u] \\
C' &= C^\top
\end{aligned}$$

670 This further leads to $P' = P^\top$.

671 If we use an asymmetric Sinkhorn cost (e.g. $C[u, v] = \|\text{ReLU}(c_\phi(x_K(u)) - c_\phi(x'_K(v)))\|_1$), we
672 cannot ensure $C[u, v] = C'[v, u]$, which fails to satisfy $P = P^\top$.

673 **D.6 Alternative surrogate for GED**

674 From Appendix D.2, we have

$$\begin{aligned}
\text{GED}(G, G') &= \min_{P \in \mathbb{P}_N} \frac{a^\oplus + a^\ominus}{2} \left\| \max(A, PA'P^\top) \right\|_{1,1} - a^\ominus |E'| - a^\oplus |E| \\
&\quad + \frac{b^\oplus + b^\ominus}{2} \left\| \max(\eta_G, P\eta_{G'}) \right\|_1 - b^\ominus |V'| - b^\oplus |V|
\end{aligned}$$

675 Following the relaxations done in Section 3.2, we propose an alternative neural surrogate by replac-
676 ing $\|\max(A, PA'P^\top)\|_{1,1}$ by $\|\max(R, SR')\|_{1,1}$ and $\|\max(\eta_G, P\eta_{G'})\|_1$ by $\|\max(X, PX')\|_{1,1}$,
677 which gives us the approximated GED parameterized by θ and ϕ as

$$\begin{aligned}
\text{GED}_{\theta, \phi}(G, G') &= \frac{a^\oplus + a^\ominus}{2} \left\| \max(R, SR') \right\|_{1,1} - a^\ominus |E'| - a^\oplus |E| \\
&\quad + \frac{b^\oplus + b^\ominus}{2} \left\| \max(X, PX') \right\|_{1,1} - b^\ominus |V'| - b^\oplus |V| \quad (22)
\end{aligned}$$

678 We call this neural surrogate as MAX. We note that element-wise maximum over A and $PA'P^\top$,
679 only allows non-edge to non-edge mapping attribute a value of zero. However, the neural surrogate

680 described in Equation 22 fails to capture this, due to the presence of the soft alignment matrix S .
681 To address this, we explicitly discard such pairs from MAX by applying an OR operator over the
682 edge presence between concerned node pairs, derived from the adjacency matrices A and A' and
683 populated in $\text{OR}(A, A') \in \mathbb{R}^{\binom{N}{2} \times \binom{N}{2}}$ given by $\text{OR}(A[u, v], A'[u', v'])$. Similarly, the indication of
684 node presence can be given as $\text{OR}(\eta_G, \eta_{G'})[u, u'] = \text{OR}(\eta_G[u], \eta_{G'}[u'])$. Hence, we write

$$\begin{aligned} \text{GED}_{\theta, \phi}(G, G') = & \frac{a^{\oplus} + a^{\ominus}}{2} \|\text{OR}(A, A') \odot \max(R, SR')\|_{1,1} - a^{\ominus}|E'| - a^{\oplus}|E| \\ & + \frac{b^{\oplus} + b^{\ominus}}{2} \|\text{OR}(\eta_G, \eta_{G'}) \odot \max(X, PX')\|_{1,1} - b^{\ominus}|V'| - b^{\oplus}|V| \end{aligned} \quad (23)$$

685 We call this formulation as MAX-OR. We provide the comparison between MAX, MAX-OR, and
686 our models in Appendix F.

687 E Details about experimental setup

688 E.1 Generation of datasets

689 We have evaluated the performance of our methods and baselines on seven real-world datasets:
690 Mutagenicity (Mutag), Ogbg-Code2 (Code2), Ogbg-Molhiv (Molhiv), Ogbg-Molpcba (Molpcba),
691 AIDS, Linux and Yeast. We split each dataset into training, validation, and test splits in ratio of
692 60:20:20. For each split \mathcal{D} , we construct $(|\mathcal{D}|(|\mathcal{D}| + 1))/2$ source and target graph instance pairs as
693 follows: $\mathcal{S} = \{(G_i, G_j) : G_i, G_j \in \mathcal{D} \wedge i \leq j\}$. We perform experiment in *four* GED regimes:

- 694 1. GED under equal cost functions, where $b^\ominus = b^\oplus = a^\ominus = a^\oplus = 1$ and substitution costs are 0
- 695 2. GED under unequal cost functions, where $b^\ominus = 3, b^\oplus = 1, a^\ominus = 2, a^\oplus = 1$ and substitution
696 costs are 0
- 697 3. edge GED under unequal cost functions, where $b^\ominus = b^\oplus = 0, a^\ominus = 2, a^\oplus = 1$, and substitution
698 costs are 0
- 699 4. GED with node substitution under equal cost functions, where $b^\ominus = b^\oplus = a^\ominus = a^\oplus = 1$, as well
700 as the node substitution cost $b^\sim = 1$.

701 We emphasize that we generated clean datasets by filtering out isomorphic graphs from the original
702 datasets before performing the training, validation, and test splits. This step is crucial to prevent
703 isomorphism bias in the models, which can occur due to leakage between the training and testing
704 splits, as highlighted by [26].

705 For each graph, we have limited the maximum number of nodes to twenty, except for Linux, where the
706 limit is ten. Information about the datasets is summarized in Table 7. Mutag contains nitroaromatic
707 compounds, with each node having labels representing atom types. Molhiv and Molpcba contain
708 molecules with node features representing atomic number, chirality, and other atomic properties.
709 Code2 contains abstract syntax trees generated from Python codes. AIDS contains graphs of chemical
710 compounds, with node types representing different atoms. For Molhiv, Molpcba and Linux, we have
711 randomly sampled 1,000 graphs from each original dataset.

	#Graphs	# Train Pairs	# Val Pairs	# Test Pairs	Avg. $ V $	Avg. $ E $	Avg. GED equal cost	Avg. GED unequal cost
Mutag	729	95703	10585	10878	16.01	31.51	11.15	18.57
Code2	128	2926	325	378	18.77	35.53	10.02	16.43
Molhiv	1000	180300	20100	20100	15.01	31.3	11.77	19.86
Molpcba	1000	180300	20100	20100	17.52	37.35	9.58	15.73
AIDS	911	149331	16653	16836	10.97	21.94	7.38	12.07
Yeast	1000	180300	20100	20100	16.59	34.07	10.65	17.74
Linux	89	1431	153	190	8.71	16.7	4.91	7.94

Table 7: Salient characteristics of data sets.

712 E.2 Details about state-of-the-art baselines

713 We compared our model against nine state-of-the-art neural baselines and three combinatorial GED
714 baselines. Below, we provide details of the methodology and hyperparameter settings used for each
715 baseline. We ensured that the number of model parameters were in a comparable range. Specifically,
716 we set the number of GNN layers to 5, each with a node embedding dimension of 10, to ensure
717 consistency and comparability with our model. The following hyperparameters are used for training:
718 Adam optimiser with a learning rate of 0.001 and weight decay of 0.0005, batch size of 256, early
719 stopping with patience of 100 epochs, and Sinkhorn temperature set to 0.01.

720 Neural Baselines:

- 721 • **GMN-Match and GMN-Embed** Graph Matching Networks (GMN) use Euclidean distance to
722 assess the similarity between graph-level embeddings of each graph. GMN is available in two
723 variants: GMN-Embed, a late interaction model, and GMN-Match, an early interaction model. For
724 this study, we used the official implementation of GMN to compute Graph Edit Distance (GED).¹
- 725 • **ISONET** ISONET utilizes the Gumbel-Sinkhorn operator to learn asymmetric edge alignments
726 between two graphs for subgraph matching. In our study, we extend ISONET’s approach to predict

¹<https://github.com/Lin-Yijie/Graph-Matching-Networks/tree/main>

727 the Graph Edit Distance (GED) score. We utilized the official PyTorch implementation provided
728 by the authors for our experiments.²

- 729 • **GREED** GREED utilizes a siamese network architecture to compute graph-level embeddings in
730 parallel for two graphs. It calculates the Graph Edit Distance (GED) score by computing the norm
731 of the difference between these embeddings. The official implementation provided by the authors
732 was used for our experiments.³
- 733 • **ERIC** ERIC utilizes a regularizer to learn node alignment, eliminating the need for an explicit node
734 alignment module. The similarity score is computed using a Neural Tensor Network (NTN) and a
735 Multi-Layer Perceptron (MLP) applied to the final graph-level embeddings of both graphs. These
736 embeddings are derived by concatenating graph-level embeddings from each layer of a Graph
737 Isomorphism Network (GIN). The model is trained using a combined loss from the regularizer and
738 the predicted similarity score. For our experiments, we used the official PyTorch implementation
739 to compute the Graph Edit Distance (GED). The GED scores were inverse normalized from the
740 model output to predict the absolute GED.⁴
- 741 • **SimGNN** SimGNN leverages both graph-level and node-level embeddings at each layer of the
742 GNN. The graph-level embeddings are processed through a Neural Tensor Network to obtain a
743 pair-level embedding. Concurrently, the node-level embeddings are used to compute a pairwise
744 similarity matrix between nodes, which is then converted into a histogram feature vector. A
745 similarity score is calculated by passing the concatenation of these embeddings through a Multi-
746 Layer Perceptron (MLP). We used the official PyTorch implementation of SimGNN and inverse
747 normalization of the predicted Graph Edit Distance (GED) score to obtain the absolute GED value.⁵
- 748 • **H2MN** H2MN presents an early interaction model for graph similarity tasks. Instead of learning
749 pairwise node relations, this method attempts to find higher-order node similarity using hypergraphs.
750 At each time step of the hypergraph convolution, a subgraph matching module is employed to learn
751 cross-graph similarity. After the convolution layers, a readout function is utilized to obtain graph-
752 level embeddings. These embeddings are then concatenated and passed through a Multi-Layer
753 Perceptron (MLP) to compute the similarity score. We used the official PyTorch implementation of
754 H2MN.⁶
- 755 • **GraphSim** GraphSim uses GNN, where at each layer, a node-to-node similarity matrix is computed
756 using the node embeddings. These similarity matrices are then processed using Convolutional
757 Neural Networks (CNNs) and Multi-Layer Perceptrons (MLPs) to calculate a similarity score. We
758 utilized the official PyTorch implementation.⁷
- 759 • **EGSC** We used the Teacher model proposed by Efficient Graph Similarity Computation (EGSC),
760 which leverages an Embedding Fusion Network (EFN) at each layer of the Graph Isomorphism
761 Network (GIN). The EFN generates a single embedding from a pair of graph embeddings. The
762 embeddings of the graph pair from each layer are concatenated and subsequently passed through
763 an additional EFN layer and a Multi-Layer Perceptron (MLP) to obtain the similarity score. To
764 predict the absolute Graph Edit Distance (GED), we inversely normalized the GED score obtained
765 from the output of EGSC. We utilized the official PyTorch implementation provided by the authors
766 for our experiments.⁸

767 **Combinatorial Baselines:** We use the GEDLIB⁹ library for implementation of all combinatorial
768 baselines.

- 769 • **Bipartite [41]** Bipartite is an approximate algorithm that considers nodes and surrounding edges
770 of nodes into account try to make a bipartite matching between two graphs. They use linear
771 assignment algorithms to match nodes and their surroundings in two graphs.
- 772 • **Branch [8], Branch Tight [8]** improve upon [41] by decomposing graphs into branches. Branch
773 Tight algorithm is another version of Branch that calculates a tighter lower bound but has a higher
774 time complexity than Branch.

²<https://github.com/Indradyumna/ISONET>

³<https://github.com/idea-iitd/greed>

⁴<https://github.com/JhuoW/ERIC>

⁵<https://github.com/benedekrozemberczki/SimGNN>

⁶<https://github.com/cszhangzhen/H2MN>

⁷<https://github.com/yunshengb/GraphSim>

⁸https://github.com/canqin001/Efficient_Graph_Similarity_Computation

⁹<https://github.com/dbblumenthal/gedlib>

- 775 • **Anchor Aware GED** Chang et al. [15] provides an approximation algorithm that calculates a
776 tighter lower bound using the anchor aware technique.
- 777 • **IPFP** [11] is an approximation algorithm which handles node and edge mapping simultaneously
778 unlike previously discussed methods. This solves a quadratic assignment problem on edges and
779 nodes.
- 780 • **F2** [29] uses a binary linear programming approach to find a higher lower bound on GED calculation.
781 This method was used with a very high time limit to generate Ground truth for our experiments.

782 E.3 Details about GRAPHEDX

783 At the high level, GRAPHEDX consists of two components EMBED_θ and PERMNET_ϕ .

784 **Neural Parameterization of EMBED_θ :** EMBED_θ consists of two modules: a GNN denoted as
785 MPNN_θ and a MLP_θ . The MPNN_θ consists of $K = 5$ propagation layers used to compute node
786 embeddings of dimension $d = 10$. At each layer k , we compute the updated the node embedding as
787 follows:

$$x_{k+1}(u) = \text{UPDATE}_\theta \left(x_k(u), \sum_{v \in \text{nbr}(u)} \text{LRL}_\theta(x_k(u), x_k(v)) \right) \quad (24)$$

788 where LRL_θ is a Linear-ReLU-Linear network, with $d = 10$ features, and the UPDATE_θ network
789 consists of a Gated Recurrent Unit [30]. In case of GED setting under equal cost and GED setting
790 under unequal cost, we set the initial node features $x_0(u) = 1$, following [30]. However, in case
791 of computation of GED with node substitution costs, we explicitly provide the one-hot labels as
792 node features. Given the node embeddings and edge-presence indicator obtained from the adjacency
793 matrices, after 5 layer propagations, we compute the edge embeddings $r(e)$ using MLP_θ , which
794 is decoupled from MPNN_θ . MLP_θ consists of a Linear-ReLU-Linear network that maps the
795 $2d + 1 = 21$ dimensional input consisting of forward $(x_K(u) || x_K(v) || A[u, v])$ and backward
796 $(x_K(v) || x_K(u) || A[v, u])$ signals to $D = 20$ dimensions.

797 **Neural Parameterization of PERMNET_ϕ :** Given the node embeddings $x_K(\cdot)$ and $x'_K(\cdot)$, we first
798 pass them through a neural network c_ϕ which consists of a Linear-ReLU-Linear network transforming
799 the features from $d = 10$ to N dimensions, which is the number of nodes after padding. Except
800 for Linux where $N = 10$, all other datasets have $N = 20$. We obtain the matrix C such that
801 $C[u, u'] = \|c_\phi(x_K(u)) - c_\phi(x'_K(u'))\|_1$. Using temperature $\tau = 0.01$, we perform Sinkhorn
802 iterations on $\exp(-C/\tau)$ as follows for $T = 20$ iterations to get P :

$$P_k = \text{NORMCOL}(\text{NORMROW}(P_{k-1}))$$

803 where $P_0 = \exp(-C/\tau)$. Here $\text{NORMROW}(M)[i, j] = M[i, j] / \sum_\ell M[\ell, j]$ denotes the row normal-
804 ization function and $\text{NORMCOL}(M)[i, j] = M[i, j] / \sum_\ell M[i, \ell]$ denotes the column normaliza-
805 tion function. We note that the soft alignment P obtained does not depend on the GED cost values,
806 as discussed in Appendix D. The soft alignment P for nodes is used to construct soft alignment S for
807 as follows: $S[(u, v), (u', v')] = P[u, u']P[v, v'] + P[u, v']P[v, u']$.

808 E.4 Evaluation metrics

809 Given the dataset \mathcal{S} consisting of input pairs of graphs (G, G') along with the ground truth
810 $\text{GED}(G, G')$ and model prediction $\widehat{\text{GED}}(G, G')$, we evaluate the performance of the model us-
811 ing the Root Mean Square Error (RMSE) and Kendall-Tau (KTau) [28] between the predicted GED
812 scores and actual GED values.

- 813 • **MSE:** It evaluates how far the predicted GED values are from the ground truth. A better performing
814 model is indicated by a lower MSE value.

$$\text{MSE} = \frac{1}{|\mathcal{S}|} \sum_{(G, G') \in \mathcal{S}} \left(\text{GED}(G, G') - \widehat{\text{GED}}(G, G') \right)^2 \quad (25)$$

- 815 • **KTau:** Selection of relevant corpus graphs via graph similarity scoring is crucial to graph retrieval
816 setups. In this context, we would like the number of concordant pairs N_+ (where the ranking of
817 ground truth GED and model prediction agree) to be high, and the discordant pairs N_- (where the
818 two disagree) to be low. Formally, we write

$$\text{KTau} = \frac{N_+ - N_-}{\binom{|\mathcal{S}|}{2}} \quad (26)$$

819 For the methods which compute a similarity score between the pair of graphs through the notion of
820 normalized GED, we map the similarity score s back to the GED as $\widehat{\text{GED}}(G, G') = -\frac{|V|+|V'|}{2} \log(s +$
821 $\epsilon)$ where $\epsilon = 10^{-7}$ is added for stability of the logarithm.

822 **E.5 Hardware and license**

823 We implement our models using Python 3.11.2 and PyTorch 2.0.0. The training of our models and
824 the baselines was performed across servers containing Intel Xeon Silver 4216 2.10GHz CPUs, and
825 Nvidia RTX A6000 GPUs. Running times of all methods are compared on the same GPU.

826 **F Additional experiments**

827 In this section, we present results from various additional experiments performed to measure the
 828 performance of our model under different cost settings.

829 **F.1 Comparison of GRAPHEDX with baselines on equal and unequal cost setting**

830 Tables 8 and 9 report performance in terms of MSE under equal and unequal cost settings, respectively.
 831 Table 10 reports performance in terms of KTAU under both equal and unequal cost settings. The results
 832 are similar to those in Table 2, where our model is the clear winner across all datasets, outperforming
 833 the second-best performer by a significant margin. There is no consistent second-best model, but
 834 ERIC, EGSC, and ISONET perform comparably and better than the others.

	Mutag	Code2	Molhiv	Molpcba	AIDS	Linux	Yeast
GMN-Match	0.797 ± 0.013	1.677 ± 0.187	1.318 ± 0.020	1.073 ± 0.011	0.821 ± 0.010	0.687 ± 0.088	1.175 ± 0.013
GMN-Embed	1.032 ± 0.016	1.358 ± 0.104	1.859 ± 0.020	1.951 ± 0.020	1.044 ± 0.013	0.736 ± 0.102	1.767 ± 0.021
ISONET	1.187 ± 0.021	0.879 ± 0.061	1.354 ± 0.015	1.106 ± 0.011	1.640 ± 0.020	1.185 ± 0.115	1.578 ± 0.019
GREED	1.398 ± 0.033	1.869 ± 0.140	1.708 ± 0.019	1.550 ± 0.017	1.004 ± 0.012	1.331 ± 0.169	1.423 ± 0.015
ERIC	0.719 ± 0.011	1.363 ± 0.110	1.165 ± 0.018	0.862 ± 0.009	0.731 ± 0.008	1.664 ± 0.260	0.969 ± 0.010
SimGNN	1.471 ± 0.024	2.667 ± 0.215	1.609 ± 0.020	1.456 ± 0.020	1.455 ± 0.020	7.232 ± 0.762	1.999 ± 0.043
H2MN	1.278 ± 0.021	7.240 ± 0.527	1.521 ± 0.020	1.402 ± 0.020	1.114 ± 0.015	2.238 ± 0.247	1.353 ± 0.018
GraphSim	2.005 ± 0.031	3.139 ± 0.206	2.577 ± 0.064	1.656 ± 0.023	1.936 ± 0.026	2.900 ± 0.318	2.232 ± 0.030
EGSC	0.765 ± 0.011	4.165 ± 0.285	1.138 ± 0.016	0.938 ± 0.010	0.627 ± 0.007	2.411 ± 0.325	0.950 ± 0.010
GRAPHEDX	0.492 ± 0.007	0.429 ± 0.036	0.781 ± 0.008	0.764 ± 0.007	0.565 ± 0.006	0.354 ± 0.043	0.717 ± 0.007

Table 8: Comparison with baselines in terms of MSE including standard error for equal cost setting ($b^\ominus = b^\oplus = a^\ominus = a^\oplus = 1$). Green (yellow) numbers report the best (second best) performers.

	Mutag	Code2	Molhiv	Molpcba	AIDS	Linux	Yeast
GMN-Match	69.210 ± 0.883	13.472 ± 0.970	76.923 ± 0.862	23.985 ± 0.224	31.522 ± 0.513	21.519 ± 2.256	63.179 ± 1.127
GMN-Embed	72.495 ± 0.915	13.425 ± 1.035	78.254 ± 0.865	28.437 ± 0.268	33.221 ± 0.523	20.591 ± 2.136	60.949 ± 0.663
ISONET	3.369 ± 0.062	3.025 ± 0.206	3.451 ± 0.039	2.781 ± 0.029	5.513 ± 0.092	3.031 ± 0.299	4.555 ± 0.061
GREED	68.732 ± 0.867	11.095 ± 0.773	78.300 ± 0.795	26.057 ± 0.238	34.354 ± 0.557	20.667 ± 2.140	60.652 ± 0.704
ERIC	1.981 ± 0.032	12.767 ± 1.177	3.377 ± 0.070	2.057 ± 0.020	1.581 ± 0.017	7.809 ± 0.911	2.341 ± 0.030
SimGNN	4.747 ± 0.079	5.212 ± 0.360	4.145 ± 0.051	3.465 ± 0.047	4.316 ± 0.071	5.369 ± 0.546	4.496 ± 0.060
H2MN	3.413 ± 0.053	9.435 ± 0.728	3.782 ± 0.046	3.396 ± 0.046	3.105 ± 0.043	5.848 ± 0.611	3.678 ± 0.046
GraphSim	5.370 ± 0.092	7.405 ± 0.577	6.643 ± 0.181	3.928 ± 0.053	5.266 ± 0.081	6.815 ± 0.628	6.907 ± 0.137
EGSC	1.758 ± 0.026	3.957 ± 0.365	2.371 ± 0.025	2.133 ± 0.022	1.693 ± 0.023	5.503 ± 0.496	2.157 ± 0.027
GRAPHEDX	1.134 ± 0.016	1.478 ± 0.118	1.804 ± 0.019	1.677 ± 0.016	1.252 ± 0.014	0.914 ± 0.110	1.603 ± 0.016

Table 9: Comparison with baselines in terms of MSE including standard error for unequal cost setting ($b^\ominus = 3, b^\oplus = 1, a^\ominus = 2, a^\oplus = 1$). Green (yellow) numbers report the best (second best) performers.

	GED with equal cost							GED with unequal cost						
	Mutag	Code2	Molhiv	Molpcba	AIDS	Linux	Yeast	Mutag	Code2	Molhiv	Molpcba	AIDS	Linux	Yeast
GMN-Match	0.901	0.876	0.887	0.797	0.824	0.826	0.852	0.606	0.781	0.619	0.596	0.611	0.438	0.610
GMN-Embed	0.887	0.892	0.856	0.723	0.796	0.815	0.815	0.603	0.790	0.607	0.534	0.601	0.531	0.573
ISONET	0.885	0.918	0.878	0.793	0.756	0.786	0.827	0.887	0.908	0.875	0.817	0.755	0.776	0.834
GREED	0.873	0.878	0.859	0.757	0.807	0.756	0.832	0.614	0.812	0.598	0.547	0.596	0.522	0.582
ERIC	0.909	0.892	0.897	0.820	0.837	0.736	0.868	0.620	0.804	0.895	0.841	0.855	0.633	0.886
SimGNN	0.871	0.856	0.877	0.776	0.775	0.377	0.834	0.862	0.874	0.872	0.804	0.768	0.731	0.843
H2MN	0.878	0.711	0.879	0.781	0.794	0.664	0.848	0.873	0.813	0.875	0.804	0.792	0.681	0.851
GraphSim	0.847	0.839	0.856	0.756	0.730	0.601	0.810	0.851	0.844	0.851	0.784	0.744	0.656	0.824
EGSC	0.906	0.815	0.896	0.809	0.850	0.664	0.868	0.912	0.894	0.900	0.836	0.858	0.696	0.884
GRAPHEDX	0.926	0.937	0.910	0.831	0.857	0.882	0.886	0.929	0.932	0.912	0.858	0.871	0.875	0.898

Table 10: Comparison with baselines in terms of KTAU for both equal and unequal cost settings, where for equal cost settings costs are $b^\ominus = b^\oplus = a^\ominus = a^\oplus = 1$ and for unequal cost settings costs are $b^\ominus = 3, b^\oplus = 1, a^\ominus = 2, a^\oplus = 1$. Green (yellow) numbers report the best (second best) performers.

835 **F.2 Comparison of GRAPHEdX with baselines with node substitution cost**

836 In Tables 11 and 12, we compare the performance of GRAPHEdX with baselines under a node
 837 substitution cost b^\sim . The cost setting is $b^\ominus = b^\oplus = b^\sim = a^\ominus = a^\oplus = 1$. This experiment includes
 838 only five datasets where node labels are present. We observe that GRAPHEdX outperforms all other
 839 baselines. There is no clear second-best model, but ERIC, EGSC, and ISONET perform better than
 840 the others.

	Mutag	Code2	Molhiv	Molpcba	AIDS
GMN-Match	1.057 ± 0.011	5.224 ± 0.404	1.388 ± 0.018	1.432 ± 0.017	0.868 ± 0.007
GMN-Embed	2.159 ± 0.026	4.070 ± 0.318	3.523 ± 0.040	4.657 ± 0.054	1.818 ± 0.014
ISONET	0.876 ± 0.008	1.129 ± 0.084	1.617 ± 0.020	1.332 ± 0.014	1.142 ± 0.010
GREED	2.876 ± 0.032	4.983 ± 0.531	2.923 ± 0.033	3.902 ± 0.044	2.175 ± 0.016
ERIC	0.886 ± 0.009	6.323 ± 0.683	1.537 ± 0.018	1.278 ± 0.014	1.602 ± 0.036
SimGNN	1.160 ± 0.013	5.909 ± 0.490	1.888 ± 0.031	2.172 ± 0.050	1.418 ± 0.020
H2MN	1.277 ± 0.014	6.783 ± 0.587	1.891 ± 0.024	1.666 ± 0.021	1.290 ± 0.011
GraphSim	1.043 ± 0.010	4.708 ± 0.425	1.817 ± 0.021	1.748 ± 0.021	1.561 ± 0.021
EGSC	0.776 ± 0.008	8.742 ± 0.831	1.273 ± 0.016	1.426 ± 0.018	1.270 ± 0.028
GRAPHEdX	0.441 ± 0.004	0.820 ± 0.092	0.792 ± 0.009	0.846 ± 0.009	0.538 ± 0.003

Table 11: Comparison with baselines in terms of MSE including standard error, in presence of the node substitution cost, which set to one in equal cost setting: $b^\ominus = b^\oplus = b^\sim = a^\ominus = a^\oplus = 1$. Green (yellow) numbers report the best (second best) performers.

	Mutag	Code2	Molhiv	Molpcba	AIDS
GMN-Match	0.895	0.811	0.881	0.809	0.839
GMN-Embed	0.847	0.845	0.796	0.684	0.767
ISONET	0.906	0.925	0.868	0.815	0.812
GREED	0.827	0.829	0.822	0.710	0.746
ERIC	0.905	0.847	0.872	0.818	0.815
SimGNN	0.891	0.836	0.864	0.797	0.810
H2MN	0.886	0.818	0.858	0.789	0.802
GraphSim	0.896	0.846	0.860	0.782	0.795
EGSC	0.912	0.802	0.885	0.821	0.832
GRAPHEdX	0.936	0.945	0.913	0.856	0.874

Table 12: Comparison with baselines in terms of K τ , in presence of the node substitution cost, which set to one in equal cost setting: $b^\ominus = b^\oplus = b^\sim = a^\ominus = a^\oplus = 1$. Green (yellow) numbers report the best (second best) performers.

841 **F.3 Performance evaluation for edge-only vs. all-node-pair representations**

842 Tables 13 and 14 contain extended results from Table 4 across seven datasets. The results are
 843 similar to those discussed in the main paper: (1) The all-node-pair representation performs better
 844 than the variants of edge-only representations. (2) within the edge-only representation, Edge-only
 845 (edge \rightarrow edge) performs better than Edge-only (pair \rightarrow pair) in most of the cases.

	Mutag	Code2	Molhiv	Molpcba	AIDS	Linux	Yeast
Edge-only (edge \rightarrow edge)	0.566 ± 0.008	0.683 ± 0.051	0.858 ± 0.009	0.791 ± 0.008	0.598 ± 0.006	0.454 ± 0.063	0.749 ± 0.007
Edge-only (pair \rightarrow pair)	0.596 ± 0.008	0.760 ± 0.058	0.862 ± 0.009	0.811 ± 0.008	0.606 ± 0.006	0.474 ± 0.056	0.761 ± 0.008
GRAPHEdX	0.492 ± 0.007	0.429 ± 0.036	0.781 ± 0.008	0.764 ± 0.007	0.565 ± 0.006	0.354 ± 0.043	0.717 ± 0.007

Table 13: Comparison of using all-node-pairs against edge-only representations using MSE for equal cost setting. Green (yellow) numbers report the best (second best) performers.

	Mutag	Code2	Molhiv	Molpcba	AIDS	Linux	Yeast
Edge-only (edge \rightarrow edge)	1.274 ± 0.017	1.817 ± 0.141	1.847 ± 0.019	1.793 ± 0.017	1.318 ± 0.014	0.907 ± 0.129	1.649 ± 0.016
Edge-only (pair \rightarrow pair)	1.276 ± 0.017	1.879 ± 0.136	1.865 ± 0.020	1.779 ± 0.017	1.422 ± 0.015	0.992 ± 0.114	1.694 ± 0.017
GRAPHEdX	1.134 ± 0.016	1.478 ± 0.118	1.804 ± 0.019	1.677 ± 0.016	1.252 ± 0.014	0.914 ± 0.110	1.603 ± 0.016

Table 14: Comparison of using all-node-pairs against edge-only representations using MSE for unequal cost setting. Green (yellow) numbers report the best (second best) performers.

846 **F.4 Effect of using cost-guided scoring function on baselines**

847 In Tables 15 and 16, we report the impact of replacing the baselines’ scoring function with our
 848 proposed cost-guided scoring function on three baselines across seven datasets for equal and unequal
 849 cost settings, respectively. We notice that similar to the results reported in Section 4.2, the cost-guided
 850 scoring function helps the baselines perform significantly better in both the cost settings.

	Mutag	Code2	Molhiv	Molpcba	AIDS	Linux	Yeast
GMN-Match	0.797 ± 0.013	1.677 ± 0.187	1.318 ± 0.020	1.073 ± 0.011	0.821 ± 0.010	0.687 ± 0.088	1.175 ± 0.013
GMN-Match *	0.654 ± 0.011	0.960 ± 0.092	1.008 ± 0.011	0.858 ± 0.009	0.601 ± 0.007	0.590 ± 0.084	0.849 ± 0.009
GMN-Embed	1.032 ± 0.016	1.358 ± 0.104	1.859 ± 0.020	1.951 ± 0.020	1.044 ± 0.013	0.736 ± 0.102	1.767 ± 0.021
GMN-Embed *	1.011 ± 0.017	1.179 ± 0.098	1.409 ± 0.015	1.881 ± 0.019	0.849 ± 0.010	0.577 ± 0.094	1.600 ± 0.017
GREED	1.398 ± 0.033	1.869 ± 0.140	1.708 ± 0.019	1.550 ± 0.017	1.004 ± 0.012	1.331 ± 0.169	1.423 ± 0.015
GREED *	2.133 ± 0.037	1.850 ± 0.156	1.644 ± 0.019	1.623 ± 0.017	1.143 ± 0.015	1.297 ± 0.151	1.440 ± 0.016
GRAPHEDX	0.492 ± 0.007	0.429 ± 0.036	0.781 ± 0.008	0.764 ± 0.007	0.565 ± 0.006	0.354 ± 0.043	0.717 ± 0.007

Table 15: Impact of cost-guided distance on MSE in equal cost setting ($b^\ominus = b^\oplus = a^\ominus = a^\oplus = 1$). * represents the variant of the baseline with cost-guided distance. Green shows the best performing model. Bold font indicates the best variant of the baseline.

	Mutag	Code2	Molhiv	Molpcba	AIDS	Linux	Yeast
GMN-Match	69.210 ± 0.883	13.472 ± 0.970	76.923 ± 0.862	23.985 ± 0.224	31.522 ± 0.513	21.519 ± 2.256	63.179 ± 1.127
GMN-Match *	1.592 ± 0.027	2.906 ± 0.285	2.162 ± 0.024	1.986 ± 0.021	1.434 ± 0.017	1.596 ± 0.211	2.036 ± 0.022
GMN-Embed	72.495 ± 0.915	13.425 ± 1.035	78.254 ± 0.865	28.437 ± 0.268	33.221 ± 0.523	20.591 ± 2.136	60.949 ± 0.663
GMN-Embed *	2.368 ± 0.039	3.272 ± 0.289	3.413 ± 0.037	4.286 ± 0.043	2.046 ± 0.025	1.495 ± 0.200	3.850 ± 0.042
GREED	68.732 ± 0.867	11.095 ± 0.773	78.300 ± 0.795	26.057 ± 0.238	34.354 ± 0.557	20.667 ± 2.140	60.652 ± 0.704
GREED *	2.456 ± 0.040	5.429 ± 0.517	3.827 ± 0.043	3.807 ± 0.040	2.282 ± 0.028	2.894 ± 0.394	3.506 ± 0.038
GRAPHEDX	1.134 ± 0.016	1.478 ± 0.118	1.804 ± 0.019	1.677 ± 0.016	1.252 ± 0.014	0.914 ± 0.110	1.603 ± 0.016

Table 16: Impact of cost-guided distance on MSE in unequal cost setting ($b^\ominus = 3, b^\oplus = 1, a^\ominus = 2, a^\oplus = 1$). * represents the variant of the baseline with cost-guided distance. Green shows the best performing model. Bold font indicates the best variant of the baseline.

851 **F.5 Results on performance of the alternate surrogates for GED**

852 In Table 17, we present the performance of the alternate surrogates scoring function for GED
 853 discussed in D under unequal cost settings ($b^\ominus = 3, b^\oplus = 1, a^\ominus = 2, a^\oplus = 1$). From the results,
 854 we can infer that the alternate surrogates have comparable performance to GRAPHEDX however
 855 GRAPHEDX outperforms it by a small margin on six out of the seven datasets.

	Mutag	Code2	Molhiv	Molpcba	AIDS	Linux	Yeast
MAX-OR	1.194 ± 0.016	1.112 ± 0.084	1.987 ± 0.022	1.806 ± 0.017	1.347 ± 0.014	1.009 ± 0.132	1.686 ± 0.018
MAX	1.351 ± 0.018	1.772 ± 0.122	1.972 ± 0.021	1.764 ± 0.017	1.346 ± 0.015	1.435 ± 0.169	1.748 ± 0.018
GRAPHEDX	1.134 ± 0.016	1.478 ± 0.118	1.804 ± 0.019	1.677 ± 0.016	1.252 ± 0.014	0.914 ± 0.110	1.603 ± 0.016

Table 17: Comparison of MSE between our variant MAX-OR and MAX. Green (yellow) numbers report the best (second best) performers.

856 **F.6 Importance of node-edge consistency**

857 GRAPHEDX enforces consistency between node and edge alignments by design. However, one might
 858 choose to enforce node-edge consistency through alignment regularization between independently
 859 learnt soft node and edge alignment. However, as shown in Figure 18, we notice that such non-
 860 constrained learning might lead to under-prediction or incorrect alignments. We demonstrate the
 861 importance of constraining the node-pair alignment S with the node alignment P by showing the
 862 mapping of nodes and edges between two graphs. The required edit operations for subfigure a) with
 863 the constrained S are two node additions $\{e, f\}$, one edge deletion (d, a) , and three edge additions
 864 $\{(a, f), (e, d), (e, f)\}$. Assuming that each edit costs one, the true GED is 6. However, in subplot b),
 865 S is not constrained, and the edit operations with the lowest cost are two node additions $\{e, f\}$ and
 866 two edge additions $\{(a, f), (e, f)\}$. This erroneously results in a GED of 4.

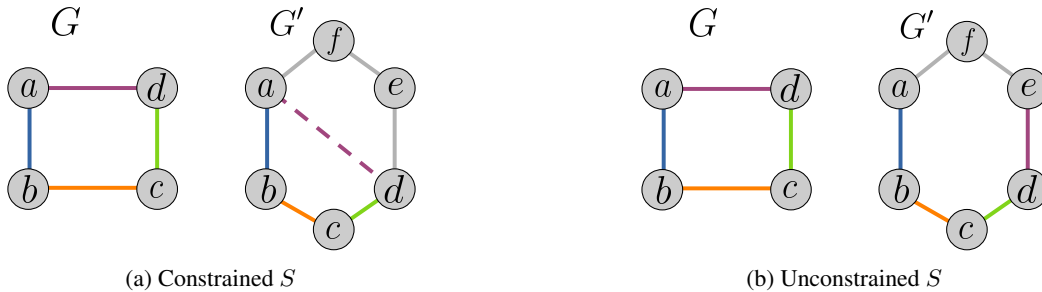


Figure 18: Node and edge alignment with constrained and unconstrained alignment S . A dashed edge represents the deleted edge. Grey edges represent added edges.

867 Further, in Table 19, we compare the performance of enforcing node-edge consistency through design
 868 (GRAPHEDX), and through alignment regularization (REG). Following the discussion in Section 3.2,
 869 such a model also exhibits a variant with XOR, called REG-xor. We notice that GRAPHEDX even
 870 outperforms such the described model in 4 out of 6 cases. We also notice that REG-xor outperforms
 871 GRAPHEDX in the other two cases. However, the above example shows a tendency to learn wrong
 alignments which in turn gives wrong optimal edit paths.

	GED with equal cost			GED with unequal cost		
	Mutag	Code2	Molhiv	Mutag	Code2	Molhiv
REG	0.536	0.576	0.848	1.162	1.488	1.877
REG-xor	0.513	0.587	0.826	1.309	1.440	1.711
GRAPHEDX	0.492	0.429	0.781	1.134	1.478	1.804

Table 19: Comparison of alignment regularizer usage versus no alignment regularizer usage on equal cost GED, Measured by MSE. Green (yellow) numbers report the best (second best) performers.

872

873 **F.7 Comparison of nine possible combinations our proposed set distances**

874 In Tables 20 and 21, we compare the performance of nine possible combinations our proposed set
 875 distances for equal and unequal cost settings respectively. Results follow the observations in Table 5,
 876 where the variant with XOR-DiffAlign outperforms those without it.

Edge edit	Node edit	Mutag	Code2	Molhiv	Molpcba	AIDS	Linux	Yeast
DiffAlign	DiffAlign	0.579 ± 0.0078	0.740 ± 0.0585	0.820 ± 0.0086	0.778 ± 0.0075	0.603 ± 0.0063	0.494 ± 0.0528	0.728 ± 0.0071
DiffAlign	AlignDiff	0.557 ± 0.0073	0.742 ± 0.0612	0.806 ± 0.0088	0.779 ± 0.0076	0.597 ± 0.0063	0.452 ± 0.0614	0.747 ± 0.0078
DiffAlign	XOR	0.538 ± 0.0072	0.719 ± 0.0560	0.794 ± 0.0083	0.777 ± 0.0075	0.580 ± 0.0060	0.356 ± 0.0512	0.750 ± 0.0075
AlignDiff	DiffAlign	0.537 ± 0.0072	0.513 ± 0.0367	0.815 ± 0.0085	0.773 ± 0.0074	0.606 ± 0.0064	0.508 ± 0.0607	0.731 ± 0.0073
AlignDiff	AlignDiff	0.578 ± 0.0079	0.929 ± 0.0659	0.833 ± 0.0086	0.773 ± 0.0075	0.593 ± 0.0062	0.605 ± 0.0678	0.761 ± 0.0076
AlignDiff	XOR	0.533 ± 0.0074	0.826 ± 0.0565	0.812 ± 0.0083	0.780 ± 0.0074	0.575 ± 0.0060	0.507 ± 0.0568	0.889 ± 0.0138
XOR	AlignDiff	0.492 ± 0.0066	0.429 ± 0.0355	0.788 ± 0.0084	0.766 ± 0.0074	0.565 ± 0.0062	0.416 ± 0.0494	0.730 ± 0.0072
XOR	DiffAlign	0.510 ± 0.0067	0.634 ± 0.0522	0.781 ± 0.0084	0.765 ± 0.0073	0.574 ± 0.0060	0.332 ± 0.0430	0.717 ± 0.0072
XOR	XOR	0.530 ± 0.0074	1.588 ± 0.1299	0.807 ± 0.0084	0.764 ± 0.0073	0.564 ± 0.0059	0.354 ± 0.0427	0.721 ± 0.0076
GRAPHEDX		0.492 ± 0.0066	0.429 ± 0.0355	0.781 ± 0.0084	0.764 ± 0.0073	0.565 ± 0.0062	0.354 ± 0.0427	0.717 ± 0.0072

Table 20: Comparison of MSE for nine combinations of our neural set distance surrogates under equal cost settings. The GRAPHEDX model was selected based on the best MSE on the validation set, while the reported results represent MSE on the test set. Green (yellow) numbers report the best (second best) performers.

Edge edit	Node edit	Mutag	Code2	Molhiv	Molpcba	AIDS	Linux	Yeast
DiffAlign	DiffAlign	1.205 ± 0.0159	2.451 ± 0.2141	1.855 ± 0.0197	1.825 ± 0.0178	1.417 ± 0.0146	0.988 ± 0.1269	1.630 ± 0.0161
DiffAlign	AlignDiff	1.211 ± 0.0164	2.116 ± 0.1581	1.887 ± 0.0199	1.811 ± 0.0174	1.319 ± 0.0140	1.078 ± 0.1168	1.791 ± 0.0185
DiffAlign	XOR	1.146 ± 0.0154	1.896 ± 0.1487	1.802 ± 0.0188	1.822 ± 0.0176	1.381 ± 0.0148	1.049 ± 0.1182	1.737 ± 0.0172
AlignDiff	DiffAlign	1.185 ± 0.0159	1.689 ± 0.1210	1.874 ± 0.0202	1.758 ± 0.0169	1.391 ± 0.0145	0.914 ± 0.1099	1.643 ± 0.0163
AlignDiff	AlignDiff	1.338 ± 0.0178	1.488 ± 0.1222	1.903 ± 0.0204	1.859 ± 0.0179	1.326 ± 0.0141	1.258 ± 0.1335	1.731 ± 0.0171
AlignDiff	XOR	1.196 ± 0.0164	1.741 ± 0.1151	1.870 ± 0.0196	1.815 ± 0.0174	1.374 ± 0.0146	1.128 ± 0.1330	1.802 ± 0.0194
XOR	AlignDiff	1.134 ± 0.0158	1.478 ± 0.1178	1.872 ± 0.0202	1.742 ± 0.0168	1.252 ± 0.0136	1.073 ± 0.1211	1.639 ± 0.0162
XOR	DiffAlign	1.148 ± 0.0157	1.489 ± 0.1220	1.804 ± 0.0192	1.757 ± 0.0171	1.340 ± 0.0140	0.931 ± 0.1149	1.603 ± 0.0160
XOR	XOR	1.195 ± 0.0172	2.507 ± 0.1979	1.855 ± 0.0195	1.677 ± 0.0161	1.319 ± 0.0141	1.193 ± 0.1490	1.638 ± 0.0169
GRAPHEDX		1.134 ± 0.0158	1.478 ± 0.1178	1.804 ± 0.0192	1.677 ± 0.0161	1.252 ± 0.0136	0.914 ± 0.1099	1.603 ± 0.0160

Table 21: Comparison of MSE for nine combinations under unequal cost settings. The GRAPHEDX model was selected based on the best MSE on the validation set, while the reported results represent MSE on the test set. Green (yellow) numbers report the best (second best) performers.

877 **F.8 Comparison of performance of GRAPHEDX on unequal cost Edge-GED**

878 We consider another cost setting – where the node costs are explicitly set to 0, and $a^\oplus = 1, a^\ominus = 2$.
 879 In such a case, GRAPHEDX only consists of $\Delta^\ominus(R, R' | S)$ and $\Delta^\oplus(R, R' | S)$ terms. To showcase
 880 the importance of aligning edges through edge alignment, we generate an alternate model, where the
 881 alignment happens through the terms $\Delta^\ominus(X, X' | P)$ and $\Delta^\oplus(X, X' | P)$, where we set $b^\oplus = 1$ and
 882 $b^\ominus = 2$, and set the edge costs to 0. We call this model NodeSwap (w/o XOR), and the corresponding
 883 XOR variant as NodeSwap + XOR. In Table 22, we compare the performance variants of GRAPHEDX
 884 with NodeSwap (w/o XOR) and the rest of the baselines to predict the Edge GED score in an unequal
 885 cost setting. From the results, we can infer that the performance of edge-alignment based model to
 predict Edge-GED outperforms the corresponding node-alignment version.

	MSE \pm STD			Ktau		
	Mutag	Molhiv	Linux	Mutag	Molhiv	Linux
GMN-Match	11.276 \pm 0.143	13.586 \pm 0.171	4.893 \pm 0.527	0.600	0.562	0.453
GMN-Embed	13.627 \pm 0.179	16.482 \pm 0.188	4.363 \pm 0.420	0.556	0.529	0.484
ISONET	1.468 \pm 0.020	2.142 \pm 0.023	1.930 \pm 0.186	0.846	0.802	0.659
GREED	11.906 \pm 0.148	13.723 \pm 0.136	3.847 \pm 0.397	0.588	0.558	0.512
ERIC	1.900 \pm 0.028	2.154 \pm 0.024	3.361 \pm 0.353	0.823	0.805	0.510
SimGNN	3.138 \pm 0.052	3.771 \pm 0.046	5.089 \pm 0.524	0.784	0.736	0.410
H2MN	3.771 \pm 0.062	3.735 \pm 0.047	5.443 \pm 0.566	0.748	0.741	0.358
GraphSim	4.696 \pm 0.076	5.200 \pm 0.074	6.597 \pm 0.697	0.720	0.694	0.316
EGSC	1.871 \pm 0.028	2.187 \pm 0.025	2.803 \pm 0.260	0.823	0.797	0.608
NodeSwap (w/o XOR)	1.246 \pm 0.017	1.858 \pm 0.019	0.997 \pm 0.124	0.857	0.814	0.757
NodeSwap + XOR	11.984 \pm 0.227	11.158 \pm 0.196	10.959 \pm 1.116	0.586	0.604	0.321
GRAPHEDX (w/o XOR)	1.174 \pm 0.016	1.842 \pm 0.019	0.976 \pm 0.115	0.863	0.815	0.764
GRAPHEDX + XOR	1.125 \pm 0.016	1.855 \pm 0.020	0.922 \pm 0.108	0.866	0.817	0.780

Table 22: Comparison of edge-alignment based GED scoring function with node-alignment based GED scoring function and state-of-the-art baselines under the cost setting: $a^\ominus = 2, a^\oplus = 1, b^\ominus = b^\oplus = 0$. In case of NodeSwap (w/o XOR), we swap the edge costs and node costs, and expect the model to learn the alignments in Edge GED through node alignment only. **Green** (yellow) numbers report the best (second best) performers.

886

887 **E.9 Comparison of performance of our model with baselines using scatter plot**

888 In Figure 23, we illustrate the performance of our model compared to the second-best performing
 889 model, under both equal and unequal cost settings, by visualizing the distribution of outputs of the
 890 predicted GEDs by both models. We observe that predictions from our model consistently align
 891 closer to the $y = x$ line across various datasets showcasing lower output variance as compared to the
 next best-performing model.

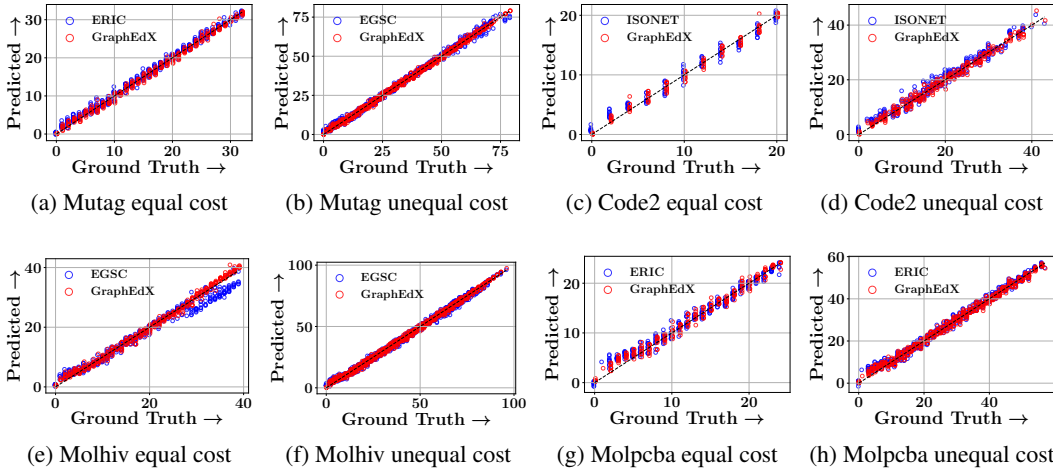


Figure 23: Scatter plot comparing the distribution of the predicted GED of our model with the next best-performing model across various datasets under both equal and unequal cost settings.

892

893 **E.10 Comparison of performance of our model with baselines using error distribution**

894 In Figure 24, we plot the distribution of error (MSE) of our model against the second-best performing
 895 model, under both equal and unequal cost settings. We observe that our model performs better,
 896 exhibiting a higher probability density for lower MSE values and a lower probability density for
 higher MSE values.

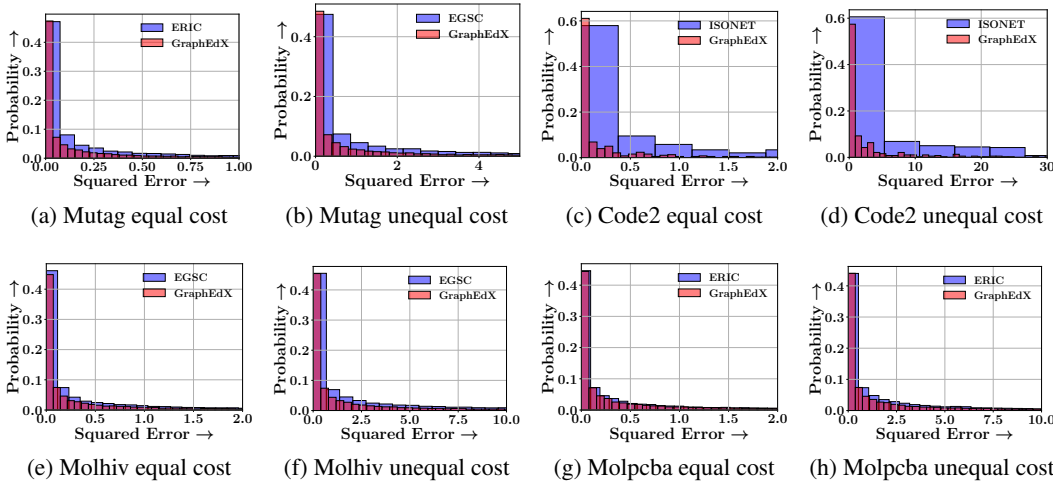


Figure 24: Error distribution of our model compared to the next best-performing model across various datasets under both equal and unequal cost settings.

897

898 **F.11 Comparison of Combinatorial Optimisation Gadgets for GED prediction**

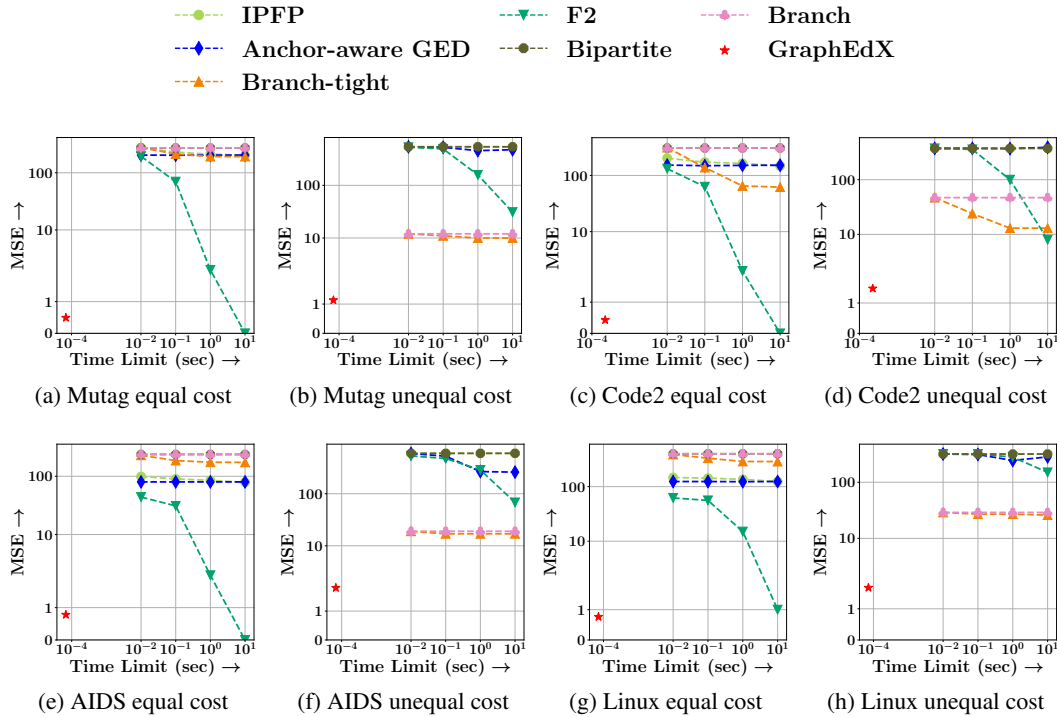


Figure 25: Performance of combinatorial optimization algorithms on various datasets under both equal and unequal cost settings is evaluated. We plot MSE against the time limit allocated to the combinatorial algorithms. Additionally, we include the amortized time of our model and its MSE.

899 We compare the runtime performance of six combinatorial optimization algorithms described in
 900 Appendix E (ipfp [11], anchor-aware GED [15], branch tight [8], F2 [29], bipartite [41] and branch
 901 [8]). We note that combinatorial algorithms are slow to approximate the GED between two graphs.
 902 Specifically, GRAPHEDX often predicts the GED in $\sim 10^{-4}$ seconds per graph, however, the
 903 performance of the combinatorial baselines are extremely poor under such a time constraint. Hence,
 904 we execute the combinatorial algorithms with four different time limits per graph: ranging from 10^{-2}
 905 seconds (100x our method) to 10 seconds (10^5 x our method).

906 In Figure 25, we depict the MSE versus time limit for the aforementioned combinatorial algorithms
 907 under both equal and unequal cost settings. We also showcase the inference time per graph of our
 908 method in the figure. It is evident that even with a time limit scaled by 10^5 x, most combinatorial
 909 algorithms struggle to achieve a satisfactory approximation for the GED.

910 **F.12 Prediction timing analysis**

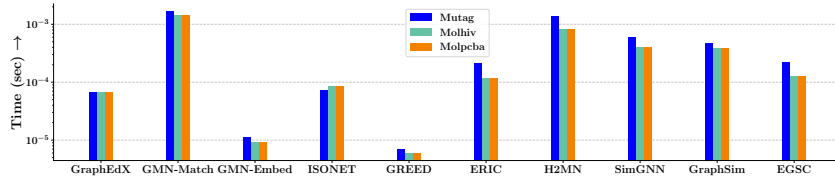


Figure 26: GED inference time comparison between our model and baselines. We notice that GRAPHEDX is consistently the third-fastest amongst all baselines. Although GMN-Embed and GREED have the lowest inference time, GRAPHEDX has much lower MSE consistently.

911 In Figure 26 illustrates the inference time per graph of our model versus under equal cost settings,
 912 averaged over ten runs. From the figure, we observe the following (1) GRAPHEDX outperforms most
 913 of the baselines in terms of inference time (2) GMN-Embed and GREED, run faster compared to
 914 all other methods due to lack of interaction between graphs, which results in poor performance at
 915 predicting the GED.

916 **F.13 Visualization (Optimal edit path) + Pseudocode**

917 In Algorithm 1, we present the pseudocode to generate the optimal edit path given the learnt node
 918 and edge alignments from GRAPHEDX. Figure 27 demonstrates how the operations in the edit path
 919 can be utilized to convert G to G' .

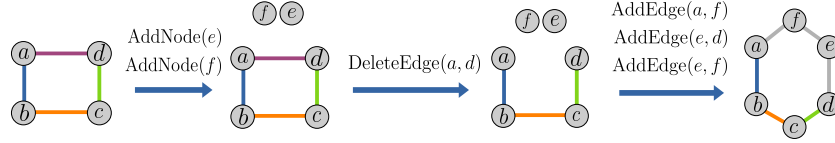


Figure 27: An example of the sequence of edit operations performed to convert one graph into another.

Algorithm 1 Generation of Edit Path

```

1: function GETEDITPATH( $G, G', \eta_G, \eta_{G'}$ )
2:    $P, S \leftarrow$  GRAPHEDX( $G, G', \eta_G, \eta_{G'}$ )
3:    $P, S \leftarrow$  HUNGARIAN( $P$ ), HUNGARIAN( $S$ )
4:    $o =$  NewList()
5:   for  $(u, v) \in [N] \times [N]$  do
6:     if  $P[u, v] = 1$  and  $\eta_G[u] = 0$  and  $\eta_{G'}[v] = 1$  then
7:       AddItem( $o, \text{ADDNODE}(u)$ )
8:     for  $(u, v), (u', v') \in \{[N] \times [N]\} \times \{[N] \times [N]\}$  do
9:       if  $S[(u, v), (u', v')] = 1$  and  $A[u, v] = 0$  and  $A'[u', v'] = 1$  then
10:        AddItem( $o, \text{ADDEDGE}((u, v))$ )
11:      if  $S[(u, v), (u', v')] = 1$  and  $A[u, v] = 1$  and  $A'[u', v'] = 0$  then
12:        AddItem( $o, \text{DELEDGE}((u, v))$ )
13:     for  $(u, v) \in [N] \times [N]$  do
14:       if  $P[u, v] = 1$  and  $\eta_G[u] = 1$  and  $\eta_{G'}[v] = 0$  then
15:         AddItem( $o, \text{DELNODE}(u)$ )
16:   return  $o$ 

```

920 **F.14 Comparison of number of parameters**

In Table 28, we present the number of parameters for each model used in the experiments.

	GMN-Match	GMN-Embed	ISONET	GREED	ERIC	SimGNN	H2MN	GraphSim	EGSC	GRAPHEDX
# Parameters	2300	2000	2595	2464	5932	1773	3004	6331	4278	3030

Table 28: Number of parameters of all methods

921

922 **NeurIPS Paper Checklist**

923 **1. Claims**

924 Question: Do the main claims made in the abstract and introduction accurately reflect the
925 paper's contributions and scope?

926 Answer: [\[Yes\]](#)

927 Justification: In Section 4, we present experiments and results to support the claims made in
928 the abstract and introduction.

929 Guidelines:

- 930 • The answer NA means that the abstract and introduction do not include the claims
931 made in the paper.
- 932 • The abstract and/or introduction should clearly state the claims made, including the
933 contributions made in the paper and important assumptions and limitations. A No or
934 NA answer to this question will not be perceived well by the reviewers.
- 935 • The claims made should match theoretical and experimental results, and reflect how
936 much the results can be expected to generalize to other settings.
- 937 • It is fine to include aspirational goals as motivation as long as it is clear that these goals
938 are not attained by the paper.

939 **2. Limitations**

940 Question: Does the paper discuss the limitations of the work performed by the authors?

941 Answer: [\[Yes\]](#)

942 Justification: In Appendix A, we discuss the limitations of our work.

943 Guidelines:

- 944 • The answer NA means that the paper has no limitation while the answer No means that
945 the paper has limitations, but those are not discussed in the paper.
- 946 • The authors are encouraged to create a separate "Limitations" section in their paper.
- 947 • The paper should point out any strong assumptions and how robust the results are to
948 violations of these assumptions (e.g., independence assumptions, noiseless settings,
949 model well-specification, asymptotic approximations only holding locally). The authors
950 should reflect on how these assumptions might be violated in practice and what the
951 implications would be.
- 952 • The authors should reflect on the scope of the claims made, e.g., if the approach was
953 only tested on a few datasets or with a few runs. In general, empirical results often
954 depend on implicit assumptions, which should be articulated.
- 955 • The authors should reflect on the factors that influence the performance of the approach.
956 For example, a facial recognition algorithm may perform poorly when image resolution
957 is low or images are taken in low lighting. Or a speech-to-text system might not be
958 used reliably to provide closed captions for online lectures because it fails to handle
959 technical jargon.
- 960 • The authors should discuss the computational efficiency of the proposed algorithms
961 and how they scale with dataset size.
- 962 • If applicable, the authors should discuss possible limitations of their approach to
963 address problems of privacy and fairness.
- 964 • While the authors might fear that complete honesty about limitations might be used by
965 reviewers as grounds for rejection, a worse outcome might be that reviewers discover
966 limitations that aren't acknowledged in the paper. The authors should use their best
967 judgment and recognize that individual actions in favor of transparency play an impor-
968 tant role in developing norms that preserve the integrity of the community. Reviewers
969 will be specifically instructed to not penalize honesty concerning limitations.

970 **3. Theory Assumptions and Proofs**

971 Question: For each theoretical result, does the paper provide the full set of assumptions and
972 a complete (and correct) proof?

973 Answer: [\[Yes\]](#)

974 Justification: In Appendix D, we provide proof for the theoretical results mentioned in the
975 paper.

976 Guidelines:

- 977 • The answer NA means that the paper does not include theoretical results.
- 978 • All the theorems, formulas, and proofs in the paper should be numbered and cross-
979 referenced.

- 980 • All assumptions should be clearly stated or referenced in the statement of any theorems.
- 981 • The proofs can either appear in the main paper or the supplemental material, but if
- 982 they appear in the supplemental material, the authors are encouraged to provide a short
- 983 proof sketch to provide intuition.
- 984 • Inversely, any informal proof provided in the core of the paper should be complemented
- 985 by formal proofs provided in appendix or supplemental material.
- 986 • Theorems and Lemmas that the proof relies upon should be properly referenced.

987 4. **Experimental Result Reproducibility**

988 Question: Does the paper fully disclose all the information needed to reproduce the main ex-
 989 perimental results of the paper to the extent that it affects the main claims and/or conclusions
 990 of the paper (regardless of whether the code and data are provided or not)?

991 Answer: [Yes]

992 Justification: We provide code and dataset in the supplementary material with instructions
 993 to reproduce the results.

994 Guidelines:

- 995 • The answer NA means that the paper does not include experiments.
- 996 • If the paper includes experiments, a No answer to this question will not be perceived
- 997 well by the reviewers: Making the paper reproducible is important, regardless of
- 998 whether the code and data are provided or not.
- 999 • If the contribution is a dataset and/or model, the authors should describe the steps taken
- 1000 to make their results reproducible or verifiable.
- 1001 • Depending on the contribution, reproducibility can be accomplished in various ways.
- 1002 For example, if the contribution is a novel architecture, describing the architecture fully
- 1003 might suffice, or if the contribution is a specific model and empirical evaluation, it may
- 1004 be necessary to either make it possible for others to replicate the model with the same
- 1005 dataset, or provide access to the model. In general, releasing code and data is often
- 1006 one good way to accomplish this, but reproducibility can also be provided via detailed
- 1007 instructions for how to replicate the results, access to a hosted model (e.g., in the case
- 1008 of a large language model), releasing of a model checkpoint, or other means that are
- 1009 appropriate to the research performed.
- 1010 • While NeurIPS does not require releasing code, the conference does require all submis-
 1011 sions to provide some reasonable avenue for reproducibility, which may depend on the
 1012 nature of the contribution. For example
- 1013 (a) If the contribution is primarily a new algorithm, the paper should make it clear how
 1014 to reproduce that algorithm.
- 1015 (b) If the contribution is primarily a new model architecture, the paper should describe
 1016 the architecture clearly and fully.
- 1017 (c) If the contribution is a new model (e.g., a large language model), then there should
 1018 either be a way to access this model for reproducing the results or a way to reproduce
 1019 the model (e.g., with an open-source dataset or instructions for how to construct
 1020 the dataset).
- 1021 (d) We recognize that reproducibility may be tricky in some cases, in which case
 1022 authors are welcome to describe the particular way they provide for reproducibility.
 1023 In the case of closed-source models, it may be that access to the model is limited in
 1024 some way (e.g., to registered users), but it should be possible for other researchers
 1025 to have some path to reproducing or verifying the results.

1026 5. **Open access to data and code**

1027 Question: Does the paper provide open access to the data and code, with sufficient instruc-
 1028 tions to faithfully reproduce the main experimental results, as described in supplemental
 1029 material?

1030 Answer: [Yes]

1031 Justification: In the supplementary material, we provide code for our model, baselines, and
 1032 experimental datasets, as well as instructions for reproducing the results.

1033 Guidelines:

- 1034 • The answer NA means that paper does not include experiments requiring code.
- 1035 • Please see the NeurIPS code and data submission guidelines ([https://nips.cc/
 1036 public/guides/CodeSubmissionPolicy](https://nips.cc/public/guides/CodeSubmissionPolicy)) for more details.
- 1037 • While we encourage the release of code and data, we understand that this might not be
 1038 possible, so “No” is an acceptable answer. Papers cannot be rejected simply for not

- 1039 including code, unless this is central to the contribution (e.g., for a new open-source
1040 benchmark).
- 1041 • The instructions should contain the exact command and environment needed to run to
1042 reproduce the results. See the NeurIPS code and data submission guidelines (<https://nips.cc/public/guides/CodeSubmissionPolicy>) for more details.
 - 1043 • The authors should provide instructions on data access and preparation, including how
1044 to access the raw data, preprocessed data, intermediate data, and generated data, etc.
 - 1045 • The authors should provide scripts to reproduce all experimental results for the new
1046 proposed method and baselines. If only a subset of experiments are reproducible, they
1047 should state which ones are omitted from the script and why.
 - 1048 • At submission time, to preserve anonymity, the authors should release anonymized
1049 versions (if applicable).
 - 1050 • Providing as much information as possible in supplemental material (appended to the
1051 paper) is recommended, but including URLs to data and code is permitted.

1052 6. Experimental Setting/Details

1053 Question: Does the paper specify all the training and test details (e.g., data splits, hyper-
1054 parameters, how they were chosen, type of optimizer, etc.) necessary to understand the
1055 results?

1056 Answer: [Yes]

1057 Justification: In Appendix E, we provide training details, such as hyperparameters and
1058 optimizer used.

1059 Guidelines:

- 1060 • The answer NA means that the paper does not include experiments.
- 1061 • The experimental setting should be presented in the core of the paper to a level of detail
1062 that is necessary to appreciate the results and make sense of them.
- 1063 • The full details can be provided either with the code, in appendix, or as supplemental
1064 material.

1065 7. Experiment Statistical Significance

1066 Question: Does the paper report error bars suitably and correctly defined or other appropriate
1067 information about the statistical significance of the experiments?

1068 Answer: [Yes]

1069 Justification: Along with Mean Squared Error we also provide Standard deviation to report
1070 the statistical significance of our results.

1071 Guidelines:

- 1072 • The answer NA means that the paper does not include experiments.
- 1073 • The authors should answer "Yes" if the results are accompanied by error bars, confi-
1074 dence intervals, or statistical significance tests, at least for the experiments that support
1075 the main claims of the paper.
- 1076 • The factors of variability that the error bars are capturing should be clearly stated (for
1077 example, train/test split, initialization, random drawing of some parameter, or overall
1078 run with given experimental conditions).
- 1079 • The method for calculating the error bars should be explained (closed form formula,
1080 call to a library function, bootstrap, etc.)
- 1081 • The assumptions made should be given (e.g., Normally distributed errors).
- 1082 • It should be clear whether the error bar is the standard deviation or the standard error
1083 of the mean.
- 1084 • It is OK to report 1-sigma error bars, but one should state it. The authors should
1085 preferably report a 2-sigma error bar than state that they have a 96% CI, if the hypothesis
1086 of Normality of errors is not verified.
- 1087 • For asymmetric distributions, the authors should be careful not to show in tables or
1088 figures symmetric error bars that would yield results that are out of range (e.g. negative
1089 error rates).
- 1090 • If error bars are reported in tables or plots, The authors should explain in the text how
1091 they were calculated and reference the corresponding figures or tables in the text.

1092 8. Experiments Compute Resources

1093 Question: For each experiment, does the paper provide sufficient information on the com-
1094 puter resources (type of compute workers, memory, time of execution) needed to reproduce
1095 the experiments?

1096 Answer: [Yes]

1098 Justification: In Appendix E we provide information on hardware used for running experi-
1099 ments.
1100 Guidelines:
1101 • The answer NA means that the paper does not include experiments.
1102 • The paper should indicate the type of compute workers CPU or GPU, internal cluster,
1103 or cloud provider, including relevant memory and storage.
1104 • The paper should provide the amount of compute required for each of the individual
1105 experimental runs as well as estimate the total compute.
1106 • The paper should disclose whether the full research project required more compute
1107 than the experiments reported in the paper (e.g., preliminary or failed experiments that
1108 didn't make it into the paper).

1109 **9. Code Of Ethics**
1110 Question: Does the research conducted in the paper conform, in every respect, with the
1111 NeurIPS Code of Ethics <https://neurips.cc/public/EthicsGuidelines?>
1112 Answer: [Yes]
1113 Justification: Yes, the research conducted in the paper conforms, in every aspect, with
1114 Neurips Code of Ethics.
1115 Guidelines:
1116 • The answer NA means that the authors have not reviewed the NeurIPS Code of Ethics.
1117 • If the authors answer No, they should explain the special circumstances that require a
1118 deviation from the Code of Ethics.
1119 • The authors should make sure to preserve anonymity (e.g., if there is a special consid-
1120 eration due to laws or regulations in their jurisdiction).

1121 **10. Broader Impacts**
1122 Question: Does the paper discuss both potential positive societal impacts and negative
1123 societal impacts of the work performed?
1124 Answer: [Yes]
1125 Justification: In Appendix B we have discuss broader impact of our work.
1126 Guidelines:
1127 • The answer NA means that there is no societal impact of the work performed.
1128 • If the authors answer NA or No, they should explain why their work has no societal
1129 impact or why the paper does not address societal impact.
1130 • Examples of negative societal impacts include potential malicious or unintended uses
1131 (e.g., disinformation, generating fake profiles, surveillance), fairness considerations
1132 (e.g., deployment of technologies that could make decisions that unfairly impact specific
1133 groups), privacy considerations, and security considerations.
1134 • The conference expects that many papers will be foundational research and not tied
1135 to particular applications, let alone deployments. However, if there is a direct path to
1136 any negative applications, the authors should point it out. For example, it is legitimate
1137 to point out that an improvement in the quality of generative models could be used to
1138 generate deepfakes for disinformation. On the other hand, it is not needed to point out
1139 that a generic algorithm for optimizing neural networks could enable people to train
1140 models that generate Deepfakes faster.
1141 • The authors should consider possible harms that could arise when the technology is
1142 being used as intended and functioning correctly, harms that could arise when the
1143 technology is being used as intended but gives incorrect results, and harms following
1144 from (intentional or unintentional) misuse of the technology.
1145 • If there are negative societal impacts, the authors could also discuss possible mitigation
1146 strategies (e.g., gated release of models, providing defenses in addition to attacks,
1147 mechanisms for monitoring misuse, mechanisms to monitor how a system learns from
1148 feedback over time, improving the efficiency and accessibility of ML).

1149 **11. Safeguards**
1150 Question: Does the paper describe safeguards that have been put in place for responsible
1151 release of data or models that have a high risk for misuse (e.g., pretrained language models,
1152 image generators, or scraped datasets)?
1153 Answer: [NA]
1154 Justification: We do not use any such dataset/method.
1155 Guidelines:
1156 • The answer NA means that the paper poses no such risks.

- 1157
- Released models that have a high risk for misuse or dual-use should be released with necessary safeguards to allow for controlled use of the model, for example by requiring that users adhere to usage guidelines or restrictions to access the model or implementing safety filters.
 - Datasets that have been scraped from the Internet could pose safety risks. The authors should describe how they avoided releasing unsafe images.
 - We recognize that providing effective safeguards is challenging, and many papers do not require this, but we encourage authors to take this into account and make a best faith effort.

1158

1159

1160

1161

1162

1163

1164

1165

1166

12. **Licenses for existing assets**

1167 Question: Are the creators or original owners of assets (e.g., code, data, models), used in the paper, properly credited and are the license and terms of use explicitly mentioned and properly respected?

1168 Answer: [Yes]

1169 Justification: We cite and provide URLs for datasets and codes that we use for the experiments.

1170 Guidelines:

- 1171
- The answer NA means that the paper does not use existing assets.
 - The authors should cite the original paper that produced the code package or dataset.
 - The authors should state which version of the asset is used and, if possible, include a URL.
 - The name of the license (e.g., CC-BY 4.0) should be included for each asset.
 - For scraped data from a particular source (e.g., website), the copyright and terms of service of that source should be provided.
 - If assets are released, the license, copyright information, and terms of use in the package should be provided. For popular datasets, paperswithcode.com/datasets has curated licenses for some datasets. Their licensing guide can help determine the license of a dataset.
 - For existing datasets that are re-packaged, both the original license and the license of the derived asset (if it has changed) should be provided.
 - If this information is not available online, the authors are encouraged to reach out to the asset's creators.

1172

1173

1174

1175

1176

1177

1178

1179

1180

1181

1182

1183

1184

1185

1186

1187

1188

1189

13. **New Assets**

1190 Question: Are new assets introduced in the paper well documented and is the documentation provided alongside the assets?

1191 Answer: [Yes]

1192 Justification: We provide our code and dataset with README file having instructions on how to run the experiments.

1193 Guidelines:

- 1194
- The answer NA means that the paper does not release new assets.
 - Researchers should communicate the details of the dataset/code/model as part of their submissions via structured templates. This includes details about training, license, limitations, etc.
 - The paper should discuss whether and how consent was obtained from people whose asset is used.
 - At submission time, remember to anonymize your assets (if applicable). You can either create an anonymized URL or include an anonymized zip file.

1195

1196

1197

1198

1199

1200

1201

1202

1203

1204

14. **Crowdsourcing and Research with Human Subjects**

1205 Question: For crowdsourcing experiments and research with human subjects, does the paper include the full text of instructions given to participants and screenshots, if applicable, as well as details about compensation (if any)?

1206 Answer: [NA]

1207 Justification: This work does not involve such research.

1208 Guidelines:

- 1209
- The answer NA means that the paper does not involve crowdsourcing nor research with human subjects.
 - Including this information in the supplemental material is fine, but if the main contribution of the paper involves human subjects, then as much detail as possible should be included in the main paper.
- 1210
- 1211
- 1212
- 1213
- 1214
- 1215

1216
1217
1218
1219
1220
1221
1222
1223
1224
1225
1226
1227
1228
1229
1230
1231
1232
1233
1234
1235
1236
1237

- According to the NeurIPS Code of Ethics, workers involved in data collection, curation, or other labor should be paid at least the minimum wage in the country of the data collector.

15. Institutional Review Board (IRB) Approvals or Equivalent for Research with Human Subjects

Question: Does the paper describe potential risks incurred by study participants, whether such risks were disclosed to the subjects, and whether Institutional Review Board (IRB) approvals (or an equivalent approval/review based on the requirements of your country or institution) were obtained?

Answer: [NA]

Justification: This work does not involve such research.

Guidelines:

- The answer NA means that the paper does not involve crowdsourcing nor research with human subjects.
- Depending on the country in which research is conducted, IRB approval (or equivalent) may be required for any human subjects research. If you obtained IRB approval, you should clearly state this in the paper.
- We recognize that the procedures for this may vary significantly between institutions and locations, and we expect authors to adhere to the NeurIPS Code of Ethics and the guidelines for their institution.
- For initial submissions, do not include any information that would break anonymity (if applicable), such as the institution conducting the review.